

---

# From Reasoning to Generalization: Knowledge-Augmented LLMs for ARC Benchmark

---

**Chao Lei, Nir Lipovetzky, Krista A. Ehinger, Yanchuan Chang**

School of Computing and Information Systems, The University of Melbourne, Australia

clei1@student.unimelb.edu.au,

{kris.ehinger, nir.lipovetzky, yanchuan.chang}@unimelb.edu.au

## Abstract

Recent reasoning-oriented LLMs have demonstrated strong performance on challenging tasks such as mathematics and science examinations. However, core cognitive faculties of human intelligence, such as abstract reasoning and generalization, remain underexplored. To address this, we evaluate recent reasoning-oriented LLMs on the Abstraction and Reasoning Corpus (ARC) benchmark, which explicitly demands both faculties. We formulate ARC as a program synthesis task and propose nine candidate solvers. Experimental results show that repeated-sampling planning-aided code generation (RSPC) achieves the highest test accuracy and demonstrates consistent generalization across most LLMs. To further improve performance, we introduce an ARC solver, Knowledge Augmentation for Abstract Reasoning (KAAR), which encodes *core knowledge* priors within an ontology that classifies priors into three hierarchical levels based on their dependencies. KAAR progressively expands LLM reasoning capacity by gradually augmenting priors at each level, and invokes RSPC to generate candidate solutions after each augmentation stage. This stage-wise reasoning reduces interference from irrelevant priors and improves LLM performance. Empirical results show that KAAR maintains strong generalization and consistently outperforms non-augmented RSPC across all evaluated LLMs, achieving around 5% absolute gains and up to 64.52% relative improvement. Despite these achievements, ARC remains a challenging benchmark for reasoning-oriented LLMs, highlighting future avenues of progress in LLMs.

## 1 Introduction

Learning from extensive training data has achieved remarkable success in major AI fields such as computer vision, natural language processing, and autonomous driving [1–3]. However, achieving human-like intelligence goes beyond learning purely from large-scale data; it requires rapid reasoning and generalizing from prior knowledge to novel tasks and situations [4]. Chollet [5] introduced Abstraction and Reasoning Corpus (ARC) to assess the generalization and abstract reasoning capabilities of AI systems. In each ARC task, the solver is required to infer generalized rules or procedures from a small set of training instances, typically fewer than five input-output image pairs, and apply them to generate output images for given input images provided in test instances (Figure 1 (a)). Each image in ARC is a pixel grid represented as a 2D matrix, where each value denotes a pixel color (Figure 1 (b)). ARC evaluates *broad generalization*, encompassing reasoning over individual input-output pairs and inferring generalized solutions via high-level abstraction, akin to inductive reasoning [6].

ARC is grounded in *core knowledge* priors, which serve as foundational cognitive faculties of human intelligence, enabling equitable comparisons between AI systems and human cognitive abilities [7]. These priors include: (1) *objectness* – aggregating elements into coherent, persistent objects; (2) *geometry and topology* – recognizing and manipulating shapes, symmetries, spatial transformations, and structural patterns (e.g., containment, repetition, projection); (3) *numbers and counting* – counting,

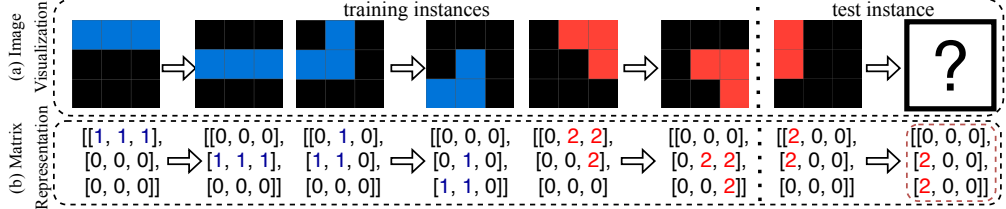


Figure 1: An ARC problem example (25ff71a9) with image visualizations (a), including three input-output pairs in the training instances, and one input image in the test instance, along with their corresponding 2D matrix representations (b). The ground-truth test output is enclosed in a red box.

sorting, comparing quantities, performing basic arithmetic, and identifying numerical patterns; and (4) *goal-directedness* – inferring purposeful transformations between initial and final states without explicit temporal cues. Incorporating these priors allows ARC solvers to replicate human cognitive processes, produce behavior aligned with human expectations, address human-relevant problems, and demonstrate human-like intelligence through generalization and abstract reasoning [5]. These features highlight ARC as a crucial benchmark for assessing progress toward general intelligence.

Chollet [5] suggested approaching ARC tasks as instances of program synthesis, which studies automatically generating a program that satisfies a high-level specification [8]. Following this proposal, recent studies [9, 10] have successfully solved partial ARC tasks by searching for program solutions encoded within object-centric domain-specific languages (DSLs). Reasoning-oriented LLMs integrate chain-of-thought (CoT) reasoning [11], often trained via reinforcement learning, further advancing program synthesis performance. Common approaches using LLMs for code generation include repeated sampling, where multiple candidate programs are generated [12], followed by best-program selection strategies [13–16], and code refinement, where initial LLM-generated code is iteratively improved using error feedback from execution results [17, 18] or LLM-generated explanations [17, 19, 18]. We note that ARC presents greater challenges than existing program synthesis benchmarks such as HumanEval [12], MBPP [20], and LiveCode [21], due to its stronger emphasis on generalization and abstract reasoning grounded in core knowledge priors, which remain underexplored. This gap motivates our evaluation of recent reasoning-oriented LLMs on the ARC benchmark, and our proposed knowledge augmentation approach to improve their performance.

We systematically assess how reasoning-oriented LLMs approach ARC tasks within the program synthesis framework. For each ARC problem, we begin by providing 2D matrices as input. We adopt three established program generation strategies: *direct generation*, *repeated sampling*, and *refinement*. Each strategy is evaluated under two solution representations: a text-based solution plan and Python code. When generating code solutions, we further examine two modalities: *standalone* and *planning-aided*, where a plan is generated to guide subsequent code development, following recent advances [18, 22, 23]. In total, nine ARC solvers are considered. We evaluate several reasoning-oriented LLMs, including proprietary models, GPT-03-mini [24, 25], and Gemini-2.0-Flash-Thinking (Gemini-2.0) [26], and open-source models, DeepSeek-R1-Distill-Llama-70B (DeepSeek-R1-70B) [27] and QwQ-32B [28]. Accuracy on test instances is reported as the primary metric. When evaluated on the ARC public evaluation set (400 problems), repeated-sampling planning-aided code generation (RSPC) demonstrates consistent generalization and achieves the highest test accuracy across most LLMs, 30.75% with GPT-03-mini, 16.75% with Gemini-2.0, 14.25% with QwQ-32B, and 7.75% with DeepSeek-R1-70B. We treat the most competitive ARC solver, RSPC, as the solver backbone.

Motivated by the success of manually defined priors in ARC solvers [9, 10], we propose Knowledge Augmentation for Abstract Reasoning (KAAR) for solving ARC tasks using reasoning-oriented LLMs. KAAR formalizes manually defined priors through a lightweight ontology that organizes priors into hierarchical levels based on their dependencies. It progressively augments LLMs with priors at each level via structured prompting. Specifically, core knowledge priors are introduced in stages: beginning with objectness, followed by geometry, topology, numbers, and counting, and concluding with goal-directedness. After each stage, KAAR applies the ARC solver backbone (RSPC) to generate the solution. This progressive augmentation enables LLMs to gradually expand their reasoning capabilities and facilitates stage-wise reasoning, aligning with human cognitive development [29]. Empirical results show that KAAR improves accuracy on test instances across all evaluated LLMs, achieving the largest absolute gain of 6.75% with QwQ-32B and the highest relative improvement of 64.52% with DeepSeek-R1-70B over non-augmented RSPC.

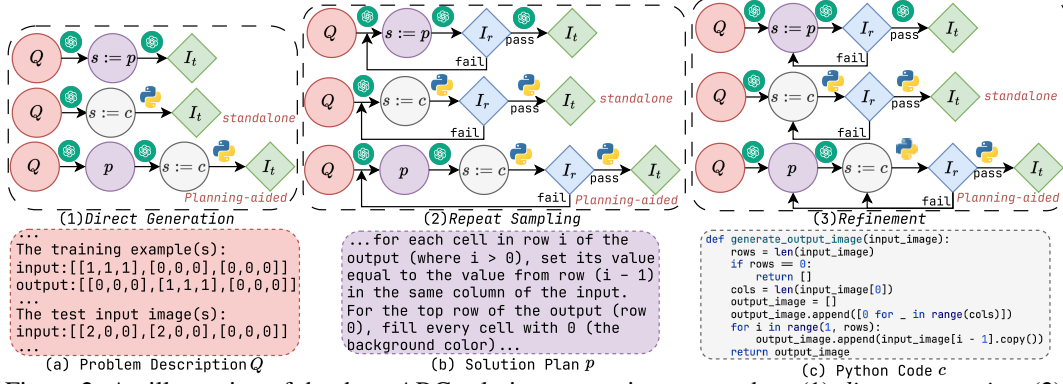


Figure 2: An illustration of the three ARC solution generation approaches, (1) *direct generation*, (2) *repeated sampling*, and (3) *refinement*, with the GPT-o3-mini input and response fragments (a–c) for solving task `25ff71a9` (Figure 1). For each approach, when the solution  $s$  is code,  $s := c$ , a plan  $p$  is either generated from the problem description  $Q$  to guide code generation (*planning-aided*) or omitted (*standalone*). Otherwise, when  $s := p$ , the plan  $p$  serves as the final solution instead.

We outline our contributions as follows:

- We evaluate the abstract reasoning and generalization capabilities of reasoning-oriented LLMs on ARC using nine solvers that differ in generation strategies, modalities, and solution representations.
- We introduce KAAR, a knowledge augmentation approach for solving ARC problems using LLMs. KAAR progressively augments LLMs with core knowledge priors structured via an ontology and applies the best ARC solver after augmenting same-level priors, further improving performance.
- We conduct a comprehensive performance analysis of the proposed ARC solvers, highlighting failure cases and remaining challenges on the ARC benchmark.

## 2 Problem Formulation

We formulate each ARC task as a tuple  $\mathcal{P} = \langle I_r, I_t \rangle$ , where  $I_r$  and  $I_t$  are sets of training and test instances. Each instance consists of an input-output image pair  $(i^i, i^o)$ , represented as 2D matrices. The goal is to leverage the LLM  $\mathcal{M}$  to generate a solution  $s$  based on training instances  $I_r$  and test input images  $\{i^i \mid (i^i, i^o) \in I_t\}$ , where  $s$  maps each test input  $i^i$  to its output  $i^o$ , i.e.,  $s(i^i) = i^o$ , for  $(i^i, i^o) \in I_t$ . We note that the test input images are visible during the generation of solution  $s$ , whereas test output images become accessible only after  $s$  is produced to validate the correctness of  $s$ . We encode the solution  $s$  in different forms, as a solution plan  $p$ , or as Python code  $c$ , optionally guided by  $p$ . We denote each ARC problem description, comprising  $I_r$  and  $\{i^i \mid (i^i, i^o) \in I_t\}$ , as  $Q$ .

## 3 ARC Solver Backbone

LLMs have shown promise in solving tasks that rely on ARC-relevant priors [30–33]. We initially assume that reasoning-oriented LLMs implicitly encode sufficient core knowledge priors to solve ARC tasks. We cast each ARC task as a program synthesis problem, which involves generating a solution  $s$  from a problem description  $Q$  without explicitly prompting for priors. We consider established LLM-based code generation approaches [17–19, 23] as candidate ARC solution generation strategies, illustrated at the top of Figure 2. These include: (1) *direct generation*, where the LLM produces the solution  $s$  in a single attempt, and then validates it on test instances  $I_t$ ; (2) *repeated sampling*, where the LLM samples solutions until one passes training instances  $I_r$ , and then evaluates it on  $I_t$ ; and (3) *refinement*, where the LLM iteratively refines an initial solution  $s$  based on failures on  $I_r$  until it succeeds, followed by evaluation on  $I_t$ . In addition, we extend the solution representation beyond code to include text-based solution plans. Given the problem description  $Q$  as input (Figure 2, block (a)), all strategies prompt the LLM to generate a solution  $s$ , represented either as a natural language plan  $p$  (block (b)),  $s := p$ , or as a Python code  $c$  (block (c)),  $s := c$ . For  $s := p$ , the solution is derived directly from  $Q$ . For  $s := c$ , we explore two modalities: the LLM either generates  $c$  directly from  $Q$  (*standalone*), or first generates a plan  $p$  for  $Q$ , which is then concatenated with  $Q$  to guide subsequent code development (*planning-aided*), a strategy widely adopted in recent work [18, 22, 23].

Repeated sampling and refinement iteratively produce new solutions based on the correctness of  $s$  on training instances  $I_r$ , and validate  $s$  on test instances  $I_t$  once it passes  $I_r$  or the iteration limit is reached. When  $s := p$ , its correctness is evaluated by prompting the LLM to generate each output image  $i^o$  given its corresponding input  $i^i$  and the solution plan  $p$ , where  $(i^i, i^o) \in I_r$  or  $(i^i, i^o) \in I_t$ . Alternatively, when  $s := c$ , its correctness is assessed by executing  $c$  on  $I_r$  or  $I_t$ . In repeated sampling, the LLM iteratively generates a new plan  $p$  and code  $c$  from the problem description  $Q$  without additional feedback. In contrast, refinement revises  $p$  and  $c$  by prompting the LLM with the previously incorrect  $p$  and  $c$ , concatenated with failed training instances. In total, nine ARC solvers are employed to evaluate the performance of reasoning-oriented LLMs on the ARC benchmark.

## 4 Knowledge Augmentation

Xu et al. [34] improved LLM performance on the ARC benchmark by prompting object-based representations for each task derived from graph-based object abstractions. Building on this insight, we propose KAAR, a knowledge augmentation approach for solving ARC tasks using reasoning-oriented LLMs. KAAR leverages Generalized Planning for Abstract Reasoning (GPAR) [10], a state-of-the-art object-centric ARC solver, to generate the core knowledge priors. GPAR encodes priors as abstraction-defined nodes enriched with attributes and inter-node relations, which are extracted using standard image processing algorithms. To align with the four knowledge dimensions in ARC, KAAR maps GPAR-derived priors into their categories. In detail, KAAR adopts fundamental abstraction methods from GPAR to enable objectness. Objects are typically defined as components based on adjacency rules and color consistency (e.g., 4-connected or 8-connected components), while also including the entire image as a component. KAAR further introduces additional abstractions: (1) *middle-vertical*, which vertically splits the image into two equal parts, and treats each as a distinct component; (2) *middle-horizontal*, which applies the same principle along the horizontal axis; (3) *multi-lines*, which segments the image using full-length rows or columns of uniform color, and treats each resulting part as a distinct component; and (4) *no abstraction*, which considers only raw 2D matrices. Under *no abstraction*, KAAR degrades to the ARC solver backbone without incorporating any priors. KAAR inherits GPAR’s geometric and topological priors, including component attributes (size, color, shape) and relations (spatial, congruent, inclusive). It further extends the attribute set with symmetry, bounding box, nearest boundary, and hole count, and augments the relation set with touching. For numeric and counting priors, KAAR follows GPAR, incorporating the largest/smallest component sizes, and the most/least frequent component colors, while extending them with statistical analysis of hole counts and symmetry, as well as the most/least frequent sizes and shapes.

GPAR approaches goal-directedness priors by searching for a sequence of program instructions [35] defined in a DSL. Each instruction supports conditionals, branching, looping, and action statements. KAAR incorporates the condition and action concepts from GPAR, and enables goal-directedness priors by augmenting LLM knowledge in two steps: 1) It prompts the LLM to identify the most relevant actions for solving the given ARC problem from ten predefined action categories (Figure 3 block (a)), partially derived from GPAR and extended based on the training set, such as color change, movement, and extension; 2) For each selected action, KAAR prompts the LLM with the associated schema to resolve implementation details. For example, for a color change action, KAAR first prompts the LLM to identify the target components (Figure 3 blocks (b)), and then specify the source and target colors for modification based on the target components (Figure 3 blocks (c)). We note that KAAR also prompts the LLM to incorporate condition-aware reasoning when determining action implementation details, using knowledge derived from geometry, topology, numbers, and counting priors. This enables fine-grained control, for example, applying color changes only to black components conditioned on the maximum or minimum size, from black (value

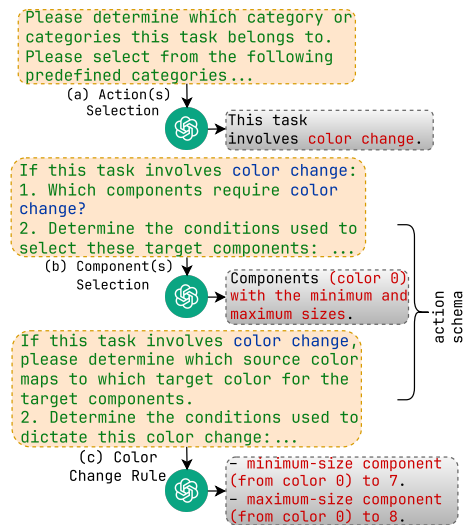


Figure 3: The example of goal-directedness priors augmentation in KAAR with input and response fragments from GPT-o3-mini.

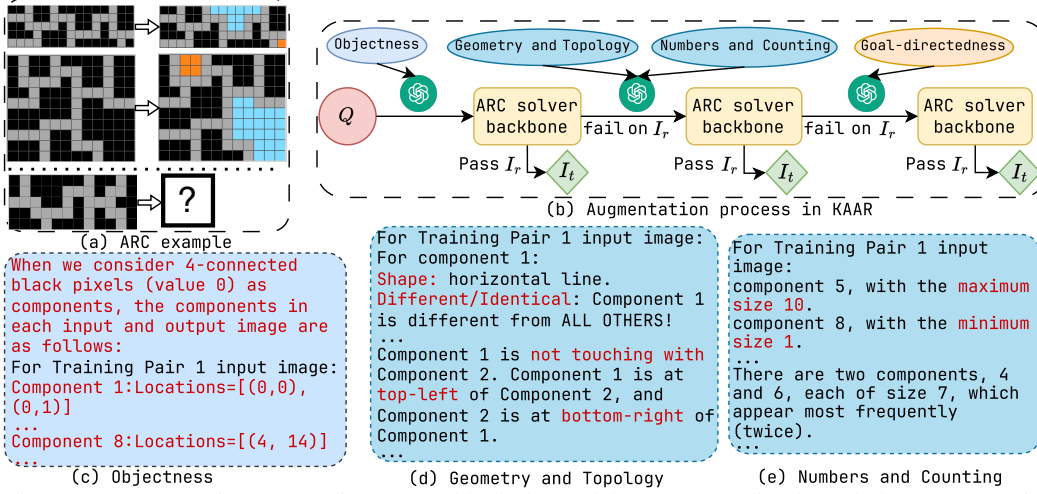


Figure 4: Augmentation process in KAAR (block (b)) and the corresponding knowledge augmentation fragments (blocks (c-e)) for ARC problem 62ab2642 (block (a)).

0) to blue (value 8) if largest, or to orange (value 7) if smallest. Figure 3 shows fragments of the goal-directedness priors augmentation. See Appendix A.2 for the full set of priors in KAAR.

KAAR encodes the full set of core knowledge priors assumed in ARC into an ontology, where priors are organized into three hierarchical levels based on their dependencies. KAAR prompts LLMs with priors at each level to enable incremental augmentation. This reduces context interference and supports stage-wise reasoning aligned with human cognitive development [29]. Figure 4, block (b), illustrates the augmentation process in KAAR alongside the augmented prior fragments used to solve the problem shown in block (a). KAAR begins augmentation with objectness priors, encoding images into components with detailed coordinates based on a specific abstraction method (block (c)). KAAR then prompts geometry and topology priors (block (d)), followed by numbers and counting priors (block (e)). These priors are ordered by dependency while residing at the same ontological level, as they all build upon objectness. Finally, KAAR augments goal-directedness priors, as shown in Figure 3, where target components are derived from objectness analysis and conditions are inferred from geometric, topological, and numerical analyses. After augmenting each level of priors, KAAR invokes the ARC solver backbone to generate solutions. If any solution passes training instances  $I_r$ , it is validated on the test instances  $I_t$ ; otherwise, augmentation proceeds to the next level of priors.

While the ontology provides a hierarchical representation of priors, it may also introduce hallucinations, such as duplicate abstractions, irrelevant component attributes or relations, and inapplicable actions. To address this, KAAR integrates restrictions from GPAR to filter out inapplicable priors. KAAR adopts GPAR’s duplicate-checking strategy, retaining only abstractions that yield distinct components by size, color, or shape, in at least one training instance. In KAAR, each abstraction is associated with a set of applicable priors. For instance, when the entire image is treated as a component, relation priors are excluded, and actions such as movement and color change are omitted, whereas symmetry and size attributes are retained and actions such as flipping and rotation are considered. In contrast, 4-connected and 8-connected abstractions include all component attributes and relations, and the full set of ten action priors. See Appendix A.3 for detailed restrictions.

## 5 Experiments

In ARC, each task is unique and solvable using only core knowledge priors [5]. We begin by comparing nine candidate solvers on the full ARC public evaluation set of 400 tasks. This offers broader insights than previous studies limited to subsets of 400 training tasks [10, 9, 36], given the greater difficulty of the evaluation set [37]. We experiment with recent reasoning-oriented LLMs, including proprietary models, GPT-03-mini and Gemini 2.0 Flash-Thinking (Gemini-2.0), and open-source models, DeepSeek-R1-Distill-Llama-70B (DeepSeek-R1-70B) and QwQ-32B. We compute accuracy on test instances  $I_t$  as the primary evaluation metric. It measures the proportion of problems where the first solution successfully solves  $I_t$  after passing the training instances  $I_r$ ; otherwise, if none pass  $I_r$  within 12 iterations, the last solution is evaluated on  $I_t$ , applied to both repeated sampling

		Direct Generation			Repeated Sampling			Refinement		
		<i>P</i>	<i>C</i>	<i>PC</i>	<i>P</i>	<i>C</i>	<i>PC</i>	<i>P</i>	<i>C</i>	<i>PC</i>
GPT-o3-mini	$I_r$	-	-	-	35.50	<b>52.50</b>	35.50	31.00	47.25	32.00
	$I_t$	20.50	24.50	22.25	23.75	<b>32.50</b>	30.75	24.75	29.25	25.75
	$I_r \& I_t$	-	-	-	22.00	<b>31.75</b>	29.25	21.75	28.50	25.00
Gemini-2.0	$I_r$	-	-	-	36.50	<b>39.50</b>	21.50	15.50	25.50	15.50
	$I_t$	7.00	6.75	6.25	10.00	14.75	<b>16.75</b>	8.75	12.00	11.75
	$I_r \& I_t$	-	-	-	9.50	14.25	<b>16.50</b>	8.00	10.50	10.75
QwQ-32B	$I_r$	-	-	-	<b>19.25</b>	13.50	15.25	16.75	15.00	14.25
	$I_t$	9.50	7.25	5.75	11.25	13.50	<b>14.25</b>	11.00	<b>14.25</b>	14.00
	$I_r \& I_t$	-	-	-	9.25	12.75	<b>13.00</b>	8.75	<b>13.00</b>	11.75
DeepSeek-R1-70B	$I_r$	-	-	-	<b>8.75</b>	6.75	7.75	6.25	5.75	7.75
	$I_t$	4.25	4.75	4.50	4.25	7.25	<b>7.75</b>	4.75	5.75	<b>7.75</b>
	$I_r \& I_t$	-	-	-	3.50	6.50	<b>7.25</b>	4.25	5.25	7.00

Table 1: Performance of nine ARC solvers measured by accuracy on  $I_r$ ,  $I_t$ , and  $I_r \& I_t$  using four reasoning-oriented LLMs. For each LLM, the highest accuracy on  $I_r$  and  $I_r \& I_t$  is in bold; the highest accuracy on  $I_t$  is in red. Accuracy is reported as a percentage.  $P$  denotes the solution plan;  $C$  and  $PC$  refer to standalone and planning-aided code generation, respectively.

		$I_r$			$I_t$			$I_r \& I_t$		
		Acc	$\Delta$	$\gamma$	Acc	$\Delta$	$\gamma$	Acc	$\Delta$	$\gamma$
GPT-o3-mini	RSPC	35.50	-	-	30.75	-	-	29.25	-	-
	KAAR	<b>40.00</b>	4.50	12.68	<b>35.00</b>	4.25	13.82	<b>33.00</b>	3.75	12.82
Gemini-2.0	RSPC	21.50	-	-	16.75	-	-	16.50	-	-
	KAAR	25.75	4.25	19.77	21.75	5.00	29.85	20.50	4.00	24.24
QwQ-32B	RSPC	15.25	-	-	14.25	-	-	13.00	-	-
	KAAR	22.25	<b>7.00</b>	45.90	21.00	<b>6.75</b>	47.37	19.25	<b>6.25</b>	48.08
DeepSeek-R1-70B	RSPC	7.75	-	-	7.75	-	-	7.25	-	-
	KAAR	12.25	4.50	<b>58.06</b>	12.75	5.00	<b>64.52</b>	11.50	4.25	<b>58.62</b>

Table 2: Comparison of RSPC (repeated-sampling planning-aided code generation) and its knowledge-augmented variant, KAAR, in terms of accuracy (Acc) on  $I_r$ ,  $I_t$ , and  $I_r \& I_t$ .  $\Delta$  and  $\gamma$  denote the absolute and relative improvements over RSPC, respectively. All values are reported as percentages. The best results for  $I_r$  and  $I_r \& I_t$  are in bold; the highest for  $I_t$  is in red.

and refinement. We also report accuracy on  $I_r$  and  $I_r \& I_t$ , measuring the percentage of problems whose solutions solve  $I_r$  and both  $I_r$  and  $I_t$ . See Appendix A.4 for parameter settings.

Table 1 reports the performance of nine ARC solvers across four reasoning-oriented LLMs. For direct generation methods, accuracy on  $I_r$  and  $I_r \& I_t$  is omitted, as solutions are evaluated directly on  $I_t$ . GPT-o3-mini consistently outperforms all other LLMs, achieving the highest accuracy on  $I_r$  (52.50%),  $I_t$  (32.50%), and  $I_r \& I_t$  (31.75%) under repeated sampling with standalone code generation ( $C$ ), highlighting its strong abstract reasoning and generalization capabilities. Notably, QwQ-32B, the smallest model, outperforms DeepSeek-R1-70B across all solvers and surpasses Gemini-2.0 under refinement. Among the nine ARC solvers, repeated sampling-based methods generally outperform those based on direct generation or refinement. This diverges from previous findings where refinement dominated conventional code generation tasks that lack abstract reasoning and generalization demands [10, 17, 19]. Within repeated sampling, planning-aided code generation ( $PC$ ) yields the highest accuracy on  $I_t$  across most LLMs. It also demonstrates the strongest generalization with GPT-o3-mini and Gemini-2.0, as evidenced by the smallest accuracy gap between  $I_r$  and  $I_r \& I_t$ , compared to solution plan ( $P$ ) and standalone code generation ( $C$ ). A similar trend is observed for QwQ-32B and DeepSeek-R1-70B, where both  $C$  and  $PC$  generalize effectively across repeated sampling and refinement. Overall, repeated sampling with planning-aided code generation, denoted as RSPC, shows the best performance and thus serves as the ARC solver backbone.

We further compare the performance of RSPC with its knowledge-augmented variant, KAAR. For each task, KAAR begins with simpler abstractions, i.e., no abstraction and whole image, and progresses to complicated 4-connected and 8-connected abstractions, consistent with GPAR. KAAR reports the accuracy on test instances  $I_t$  based on the first abstraction whose solution solves all training instances  $I_r$ ; otherwise, it records the final solution from each abstraction and selects the one that passes the most  $I_r$  to evaluate on  $I_t$ . KAAR allows the solver backbone (RSPC) up to

4 iterations per invocation, totaling 12 iterations, consistent with the non-augmented setting. See Appendix A.5 for KAAR execution details. As shown in Table 2, KAAR consistently outperforms non-augmented RSPC across all LLMs, yielding around 5% absolute gains on  $I_r$ ,  $I_t$ , and  $I_r \& I_t$ . This highlights the effectiveness and model-agnostic nature of the augmented priors. KAAR achieves the highest accuracy using GPT-o3-mini, with 40% on  $I_r$ , 35% on  $I_t$ , and 33% on  $I_r \& I_t$ . KAAR shows the greatest absolute improvements ( $\Delta$ ) using QwQ-32B and the largest relative gains ( $\gamma$ ) using DeepSeek-R1-70B across all evaluated metrics. Moreover, KAAR maintains generalization comparable to RSPC across all LLMs, indicating that the augmented priors are sufficiently abstract and expressive to serve as basis functions for reasoning, in line with ARC assumptions.

We compare relative problem coverage across evaluated LLMs under RSPC and KAAR based on successful solutions on test instances. As shown in Figure 5, each cell  $(i, j)$  represents the proportion of problems solved by the row LLM that are also solved by the column LLM. This is computed as  $\frac{|A_i \cap A_j|}{|A_i|}$ , where  $A_i$  and  $A_j$  are the sets of problems solved by the row and column LLMs, respectively. Values near 1 indicate that the column LLM covers most problems solved by the row LLM. Under RSPC (Figure 5 (a)), GPT-o3-mini exhibits broad coverage, with column values consistently above

0.85. Gemini-2.0 and QwQ-32B also show substantial alignment, with mutual coverage exceeding 0.6. In contrast, DeepSeek-R1-70B shows lower alignment, with column values below 0.45 due to fewer solved problems. Figure 5 (b) illustrates that KAAR generally improves or maintains inter-model overlap compared to RSPC. Notably, KAAR raises the minimum coverage between GPT-o3-mini and DeepSeek-R1-70B from 0.22 under RSPC to 0.34 under KAAR. These results highlight the effectiveness of KAAR in improving cross-model generalization, with all evaluated LLMs solving additional shared problems. In particular, it enables smaller models such as QwQ-32B and DeepSeek-R1-70B to better align with stronger LLMs on the ARC benchmark.

Following prior work [9, 10], we categorize 400 problems in the ARC public evaluation set into four classes based on their primary transformations: (1) *movement* (55 problems), (2) *extension* (129 problems), (3) *re-color* (115 problems), and (4) *others* (101 problems). The *others* category comprises infrequent tasks such as noise removal, selection, counting, resizing, and problems with implicit patterns that hinder systematic classification into the aforementioned categories. See Appendix A.7 for examples of each category. Figure 6 illustrates the accuracy on test instances  $I_t$  for RSPC and KAAR across four categories with evaluated LLMs. Each stacked bar represents RSPC accuracy and the additional improvement achieved by KAAR. KAAR consistently outperforms RSPC with the largest accuracy gain in *movement* (14.5% with QwQ-32B). In contrast, KAAR shows limited improvements in *extension*, since several problems involve pixel-level extension, which reduces the reliance on component-level recognition. Moreover, *extension* requires accurate spatial inference across multiple components and poses greater difficulty than *movement*, which requires mainly direction identification. Although KAAR augments spatial priors, LLMs still struggle to accurately infer positional relations among multiple components, consistent with prior findings [38–40]. Overlaps from component extensions further complicate reasoning, as LLMs often fail to recognize truncated components as unified wholes, contrary to human perceptual intuition.

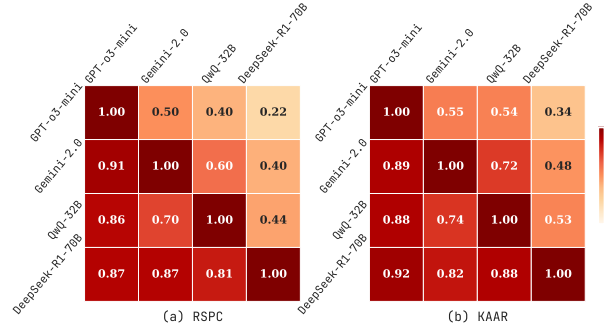


Figure 5: Asymmetric relative coverage matrices for RSPC (a) and KAAR (b), showing the proportion of problems whose test instances are solved by the row model that are also solved by the column model, across four LLMs.

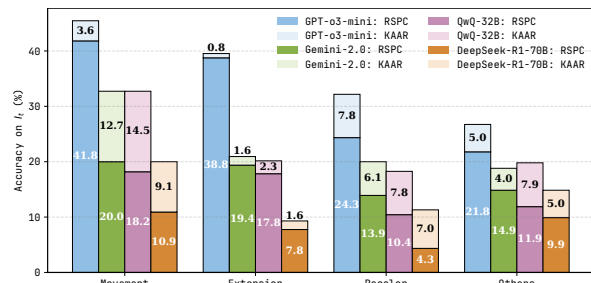


Figure 6: Accuracy on test instances  $I_t$  for RSPC and KAAR across the *movement*, *extension*, *recolor*, and *others* categories using four LLMs. Each stacked bar shows RSPC accuracy (darker segment) and the additional improvement from KAAR (lighter segment).

A notable feature of ARC is the variation in image size both within and across problems. We categorize tasks by averaging the image size per problem, computed over both training and test image pairs. We report the accuracy on  $I_t$  for RSPC and KAAR across average image size intervals using GPT-o3-mini and QwQ-32B, the strongest proprietary and open-source models in Tables 1 and 2. As shown in Figure 7, both LLMs experience performance degradation as image size increases. When the average image size exceeds 400 (20x20), GPT-o3-mini solves only three problems, while QwQ-32B solves none. In ARC, isolating relevant pixels in larger images, represented as 2D matrices, requires effective attention mechanisms in LLMs, which remains an open challenge noted in recent work [41, 34]. KAAR consistently outperforms RSPC on problems with average image sizes below 400, benefiting from object-centric representations. By abstracting each image into components, KAAR reduces interference from irrelevant pixels, directs attention to salient components, and facilitates component-level transformation analysis. However, larger images often produce both oversized and numerous components after abstraction, which continue to challenge LLMs during reasoning. Oversized components hinder transformation execution, and numerous components complicate the identification of target components.

Figure 8 presents the variance in accuracy on  $I_r$  &  $I_t$  for RSPC and KAAR as iteration count increases using GPT-o3-mini and QwQ-32B. For each task under KAAR, we include only iterations from the abstraction that solves both  $I_r$  and  $I_t$ . For KAAR, performance improvements across each 4-iteration block are driven by the solver backbone invocation after augmenting an additional level of priors: iterations 1–4 introduce objectness; 5–8 incorporate geometry, topology, numbers, and counting; 9–12 further involve goal-directedness. RSPC shows rapid improvement in the first 4 iterations and plateaus around iteration 8. At each iteration, the accuracy gap between KAAR and RSPC reflects the contribution of accumulated priors via augmentation. KAAR consistently outperforms RSPC, with the performance gap progressively increasing after new priors are augmented and peaking at iteration 12. These results highlight the benefits of KAAR. Representing core knowledge priors through a hierarchical, dependency-aware ontology enables KAAR to incrementally augment LLMs, perform stage-wise reasoning, and improve solution accuracy. Compared to augmentation at once and non-stage-wise reasoning, KAAR consistently yields superior accuracy, as detailed in Appendix A.6.

## 6 Discussion

**ARC and KAAR.** ARC serves as a visual abstract reasoning benchmark, requiring models to infer transformations from few examples for each unique task, rather than fitting to a closed rule space as in RAVEN [42] and PGM [43]. ARC assumes tasks are solvable using core knowledge priors. However, the problems are intentionally left undefined to preclude encoding complete solution rules [5]. This pushes models beyond closed-form rule fitting and toward truly domain-general capabilities. While

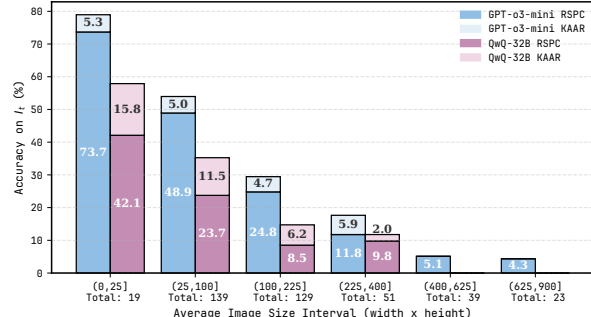


Figure 7: Accuracy on test instances  $I_t$  for RSPC and KAAR across average image size intervals, evaluated using GPT-o3-mini and QwQ-32B. See Figure 12 in Appendix for the results with the other LLMs.

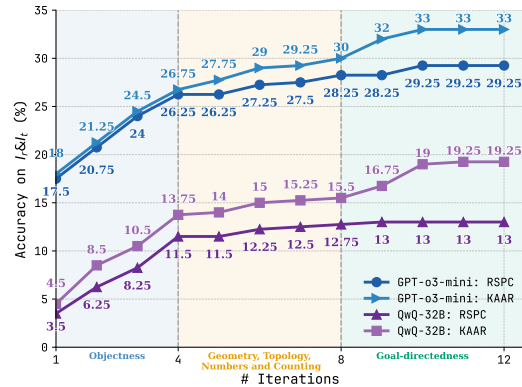


Figure 8: Variance in accuracy on  $I_r$  &  $I_t$  with increasing iterations for RSPC and KAAR using GPT-o3-mini and QwQ-32B. See Figure 13 in Appendix for the results with the other LLMs.

after the integration of goal-directedness. We note that objectness priors alone yield marginal gains with GPT-o3-mini. However, the inclusion of object attributes and relational priors (iterations 4–8) leads to improvements in KAAR over RSPC. This advantage is further amplified after the augmentation of goal-directedness priors (iterations 9–12). These results highlight the benefits of KAAR. Representing core knowledge priors through a hierarchical, dependency-aware ontology enables KAAR to incrementally augment LLMs, perform stage-wise reasoning, and improve solution accuracy. Compared to augmentation at once and non-stage-wise reasoning, KAAR consistently yields superior accuracy, as detailed in Appendix A.6.

some of the knowledge in KAAR is tailored to ARC, its central contribution lies in representing knowledge through a hierarchical, dependency-aware ontology that enables progressive augmentation. This allows LLMs to gradually expand their reasoning scope and perform stage-wise inference, improving performance on ARC without relying on an exhaustive rule set. Moreover, the ontology of KAAR is transferable to other domains requiring hierarchical reasoning, such as robotic task planning [44], image captioning [45], and visual question answering [46], where similar knowledge priors and dependencies from ARC are applicable. In KAAR, knowledge augmentation increases token consumption, while the additional tokens remain relatively constant since all priors, except goal-directedness, are generated via image processing algorithms from GPAR. On GPT-o3-mini, augmentation tokens constitute around 60% of solver backbone token usage, while on QwQ-32B, this overhead decreases to about 20%, as the solver backbone consumes more tokens. See Appendix A.8 for a detailed discussion. Incorrect abstraction selection in KAAR also leads to wasted tokens. However, accurate abstraction inference often requires validation through viable solutions, bringing the challenge back to solution generation.

**Solution Analysis.** RSPC achieves over 30% accuracy across evaluated metrics using GPT-o3-mini, even without knowledge augmentation. To assess its alignment with core knowledge priors, we manually reviewed RSPC-generated solution plans and code that successfully solve  $I_t$  with GPT-o3-mini. RSPC tends to solve problems without object-centric reasoning. For instance, in Figure 1, it shifts each row downward by one and pads the top with zeros, rather than reasoning over objectness to move each 4-connected component down by one step. Even when applying objectness, RSPC typically defaults to 4-connected abstraction, failing on the problem in Figure 9, where the test input clearly requires 8-connected abstraction. We note that object recognition in ARC involves grouping pixels into task-specific components based on clustering rules, differing from feature extraction approaches [47] in conventional computer vision tasks. Recent work seeks to bridge this gap by incorporating 2D positional encodings and object indices into Vision Transformers [41]. However, its reliance on data-driven learning weakens generalization, undermining ARC’s core objective. In contrast, KAAR enables objectness through explicitly defined abstractions, implemented via standard image processing algorithms, thus ensuring both accuracy and generalization.

**Generalization.** For all evaluated ARC solvers, accuracy on  $I_r$  consistently exceeds that on  $I_r \& I_t$ , revealing a generalization gap. Planning-aided code generation methods, such as RSPC and KAAR, exhibit smaller gaps than other solvers, though the issue persists. One reason is that solutions include low-level logic for the training pairs, thus failing to generalize. See Appendix A.9 for examples. Another reason is the usage of incorrect abstractions. For example, reliance solely on 4-connected abstraction leads RSPC to solve only  $I_r$  in Figure 9. KAAR similarly fails to generalize in this case. It selects 4-connected abstraction, the first one that solves  $I_r$ , to report accuracy on  $I_t$ , instead of the correct 8-connected abstraction, as the former is considered simpler. Table 1 also reveals that LLMs differ in their generalization across ARC solvers. While a detailed analysis of these variations is beyond the scope of this study, investigating the underlying causes could offer insights into LLM inference and alignment with intended behaviors, presenting a promising direction for future work.

## 7 Conclusion

We explored the generalization and abstract reasoning capabilities of recent reasoning-oriented LLMs on the ARC benchmark using nine candidate solvers. Experimental results show that repeated-sampling planning-aided code generation (RSPC) achieves the highest test accuracy and demonstrates consistent generalization across most evaluated LLMs. To further improve performance, we propose KAAR, which progressively augments LLMs with core knowledge priors organized into hierarchical levels based on their dependencies, and applies RSPC after augmenting each level of priors to enable stage-wise reasoning. KAAR improves LLM performance on the ARC benchmark while maintaining strong generalization compared to non-augmented RSPC. However, ARC remains challenging even for the most capable reasoning-oriented LLMs, given its emphasis on abstract reasoning and generalization, highlighting current limitations and motivating future research.

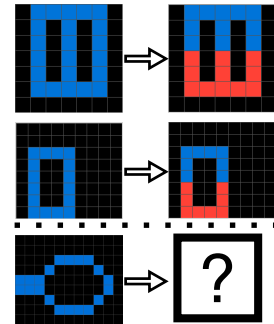


Figure 9: Fragment of ARC problem  $e7dd8335$ .

## References

- [1] Abdullah Ayub Khan, Asif Ali Laghari, and Shafique Ahmed Awan. Machine learning in computer vision: A review. *EAI Endorsed Transactions on Scalable Information Systems*, 8(32), 2021.
- [2] Daniel W Otter, Julian R Medina, and Jugal K Kalita. A survey of the usages of deep learning for natural language processing. *IEEE transactions on neural networks and learning systems*, 32(2):604–624, 2020.
- [3] Sorin Grigorescu, Bogdan Trasnea, Tiberiu Cocias, and Gigel Macesanu. A survey of deep learning techniques for autonomous driving. *Journal of field robotics*, 37(3):362–386, 2020.
- [4] Brenden M Lake, Tomer D Ullman, Joshua B Tenenbaum, and Samuel J Gershman. Building machines that learn and think like people. *Behavioral and brain sciences*, 40:e253, 2017.
- [5] François Chollet. On the measure of intelligence. *arXiv preprint arXiv:1911.01547*, 2019.
- [6] Charles S Peirce. Questions concerning certain faculties claimed for man. *The Journal of Speculative Philosophy*, 2(2):103–114, 1868.
- [7] Elizabeth S Spelke and Katherine D Kinzler. Core knowledge. *Developmental science*, 10(1):89–96, 2007.
- [8] Sumit Gulwani, Oleksandr Polozov, Rishabh Singh, et al. Program synthesis. *Foundations and Trends® in Programming Languages*, 4:1–119, 2017.
- [9] Yudong Xu, Elias B Khalil, and Scott Sanner. Graphs, constraints, and search for the abstraction and reasoning corpus. In *Proceedings of the 37th AAAI Conference on Artificial Intelligence*, AAAI, pages 4115–4122, 2023.
- [10] Chao Lei, Nir Lipovetzky, and Krista A Ehinger. Generalized planning for the abstraction and reasoning corpus. In *Proceedings of the 38th AAAI Conference on Artificial Intelligence*, AAAI, pages 20168–20175, 2024.
- [11] Jason Wei, Xuezhi Wang, Dale Schuurmans, Maarten Bosma, Fei Xia, Ed Chi, Quoc V Le, Denny Zhou, et al. Chain-of-thought prompting elicits reasoning in large language models. In *Proceedings of the 36th Advances in Neural Information Processing Systems*, NeurIPS, pages 24824–24837, 2022.
- [12] Mark Chen, Jerry Tworek, Heewoo Jun, Qiming Yuan, Henrique Ponde de Oliveira Pinto, Jared Kaplan, Harri Edwards, Yuri Burda, Nicholas Joseph, Greg Brockman, et al. Evaluating large language models trained on code. *arXiv preprint arXiv:2107.03374*, 2021.
- [13] Yujia Li, David Choi, Junyoung Chung, Nate Kushman, Julian Schrittweiser, Rémi Leblond, Tom Eccles, James Keeling, Felix Gimeno, Agustin Dal Lago, et al. Competition-level code generation with alphocode. *Science*, 378:1092–1097, 2022.
- [14] Bei Chen, Fengji Zhang, Anh Nguyen, Daoguang Zan, Zeqi Lin, Jian-Guang Lou, and Weizhu Chen. Codet: Code generation with generated tests. In *Proceedings of the 11th International Conference on Learning Representations*, ICLR, pages 1–19, 2023.
- [15] Tianyi Zhang, Tao Yu, Tatsunori Hashimoto, Mike Lewis, Wen-tau Yih, Daniel Fried, and Sida Wang. Coder reviewer reranking for code generation. In *Proceedings of the 40th International Conference on Machine Learning*, ICML, pages 41832–41846, 2023.
- [16] Ansong Ni, Srinivas Iyer, Dragomir Radev, Veselin Stoyanov, Wen-tau Yih, Sida Wang, and Xi Victoria Lin. Lever: Learning to verify language-to-code generation with execution. In *Proceedings of the 40th International Conference on Machine Learning*, ICML, pages 26106–26128, 2023.
- [17] Li Zhong, Zilong Wang, and Jingbo Shang. Debug like a human: A large language model debugger via verifying runtime execution step by step. In *Findings of the Association for Computational Linguistics: ACL 2024*, pages 851–870, 2024.

[18] Chao Lei, Yanchuan Chang, Nir Lipovetzky, and Krista A Ehinger. Planning-driven programming: A large language model programming workflow. *arXiv preprint arXiv:2411.14503*, 2024.

[19] Xinyun Chen, Maxwell Lin, Nathanael Schärli, and Denny Zhou. Teaching large language models to self-debug. In *Proceedings of the 12th International Conference on Learning Representations*, ICLR, 2024.

[20] Jacob Austin, Augustus Odena, Maxwell Nye, Maarten Bosma, Henryk Michalewski, David Dohan, Ellen Jiang, Carrie Cai, Michael Terry, Quoc Le, et al. Program synthesis with large language models. *arXiv preprint arXiv:2108.07732*, 2021.

[21] Naman Jain, King Han, Alex Gu, Wen-Ding Li, Fanjia Yan, Tianjun Zhang, Sida Wang, Armando Solar-Lezama, Koushik Sen, and Ion Stoica. Livecodebench: Holistic and contamination free evaluation of large language models for code. In *Proceedings of the 13th International Conference on Learning Representations*, ICLR, 2025.

[22] Xue Jiang, Yihong Dong, Lecheng Wang, Fang Zheng, Qiwei Shang, Ge Li, Zhi Jin, and Wenpin Jiao. Self-planning code generation with large language models. *ACM Transactions on Software Engineering and Methodology*, 33(7):1–28, 2023.

[23] Md. Ashraful Islam, Mohammed Eunus Ali, and Md Rizwan Parvez. MapCoder: Multi-agent code generation for competitive problem solving. In *Proceedings of the 62nd Annual Meeting of the Association for Computational Linguistics*, ACL, pages 4912–4944, 2024.

[24] Tianyang Zhong, Zhengliang Liu, Yi Pan, Yutong Zhang, Yifan Zhou, Shizhe Liang, Zihao Wu, Yanjun Lyu, Peng Shu, Xiaowei Yu, et al. Evaluation of openai o1: Opportunities and challenges of agi. *arXiv preprint arXiv:2409.18486*, 2024.

[25] OpenAI. Openai o3-mini. *OpenAI*, 2025. URL <https://openai.com/index/openai-o3-mini/>. Accessed: 2025-03-22.

[26] Google DeepMind. Gemini 2.0 flash thinking. *Google DeepMind*, 2024. URL <https://deepmind.google/technologies/gemini/flash-thinking/>. Accessed: 2025-03-22.

[27] Daya Guo, Dejian Yang, Haowei Zhang, Junxiao Song, Ruoyu Zhang, Runxin Xu, Qihao Zhu, Shirong Ma, Peiyi Wang, Xiao Bi, et al. Deepseek-r1: Incentivizing reasoning capability in llms via reinforcement learning. *arXiv preprint arXiv:2501.12948*, 2025.

[28] Alibaba Cloud. Alibaba cloud unveils qwq-32b: A compact reasoning model with cutting-edge performance. *Alibaba Cloud*, 2025. URL [https://www.alibabacloud.com/blog/alibaba-cloud-unveils-qwq-32b-a-compact-reasoning-model-with-cutting-edge-performance\\_602039](https://www.alibabacloud.com/blog/alibaba-cloud-unveils-qwq-32b-a-compact-reasoning-model-with-cutting-edge-performance_602039). Accessed: 2025-03-22.

[29] Zana H Babakr, Pakstan Mohamedamin, and Karwan Kakamad. Piaget’s cognitive developmental theory: Critical review. *Education Quarterly Reviews*, 2(3):517–524, 2019.

[30] Hourui Deng, Hongjie Zhang, Jie Ou, and Chaosheng Feng. Can llm be a good path planner based on prompt engineering? mitigating the hallucination for path planning. *arXiv preprint arXiv:2408.13184*, 2024.

[31] Silin Meng, Yiwei Wang, Cheng-Fu Yang, Nanyun Peng, and Kai-Wei Chang. LLM-a\*: Large language model enhanced incremental heuristic search on path planning. In *Findings of the Association for Computational Linguistics: EMNLP 2024*, pages 1087–1102, 2024.

[32] Janice Ahn, Rishu Verma, Renze Lou, Di Liu, Rui Zhang, and Wengen Yin. Large language models for mathematical reasoning: Progresses and challenges. In *Proceedings of the 18th Conference of the European Chapter of the Association for Computational Linguistics: Student Research Workshop*, EACL, pages 225–237, 2024.

[33] Yuhang Zang, Wei Li, Jun Han, Kaiyang Zhou, and Chen Change Loy. Contextual object detection with multimodal large language models. *International Journal of Computer Vision*, 133(2):825–843, 2025.

[34] Yudong Xu, Wenhao Li, Pashootan Vaezipoor, Scott Sanner, and Elias B Khalil. Llms and the abstraction and reasoning corpus: Successes, failures, and the importance of object-based representations. *arXiv preprint arXiv:2305.18354*, 2023.

[35] Chao Lei, Nir Lipovetzky, and Krista A Ehinger. Novelty and lifted helpful actions in generalized planning. In *Proceedings of the International Symposium on Combinatorial Search*, SoCS, pages 148–152, 2023.

[36] Ruocheng Wang, Eric Zelikman, Gabriel Poesia, Yewen Pu, Nick Haber, and Noah Goodman. Hypothesis search: Inductive reasoning with language models. In *Proceedings of the 12 th International Conference on Learning Representations*, ICLR, 2024.

[37] Solim LeGris, Wai Keen Vong, Brenden M Lake, and Todd M Gureckis. H-arc: A robust estimate of human performance on the abstraction and reasoning corpus benchmark. *arXiv preprint arXiv:2409.01374*, 2024.

[38] Yutaro Yamada, Yihan Bao, Andrew Kyle Lampinen, Jungo Kasai, and Ilker Yildirim. Evaluating spatial understanding of large language models. *Transactions on Machine Learning Research*, 2024.

[39] Anthony G Cohn and Jose Hernandez-Orallo. Dialectical language model evaluation: An initial appraisal of the commonsense spatial reasoning abilities of llms. *arXiv preprint arXiv:2304.11164*, 2023.

[40] Yejin Bang, Samuel Cahyawijaya, Nayeon Lee, Wenliang Dai, Dan Su, Bryan Wilie, Holly Love-nia, Ziwei Ji, Tiezheng Yu, Willy Chung, Quyet V. Do, Yan Xu, and Pascale Fung. A multitask, multilingual, multimodal evaluation of ChatGPT on reasoning, hallucination, and interactivity. In *Proceedings of the 13th International Joint Conference on Natural Language Processing and the 3rd Conference of the Asia-Pacific Chapter of the Association for Computational Linguistics*, IJCNLP-AAACL, pages 675–718, 2023.

[41] Wenhao Li, Yudong Xu, Scott Sanner, and Elias Boutros Khalil. Tackling the abstraction and reasoning corpus with vision transformers: the importance of 2d representation, positions, and objects. *arXiv preprint arXiv:2410.06405*, 2024.

[42] John Raven. The raven’s progressive matrices: change and stability over culture and time. *Cognitive psychology*, 41(1):1–48, 2000.

[43] David Barrett, Felix Hill, Adam Santoro, Ari Morcos, and Timothy Lillicrap. Measuring abstract reasoning in neural networks. In *Proceedings of the 37th International conference on machine learning*, ICML, pages 511–520, 2018.

[44] Yongcheng Cui, Ying Zhang, Cui-Hua Zhang, and Simon X Yang. Task cognition and planning for service robots. *Intelligence & Robotics*, (1):119–142, 2025.

[45] Matteo Stefanini, Marcella Cornia, Lorenzo Baraldi, Silvia Cascianelli, Giuseppe Fiameni, and Rita Cucchiara. From show to tell: A survey on deep learning-based image captioning. *IEEE transactions on pattern analysis and machine intelligence*, (1):539–559, 2022.

[46] Ngoc Dung Huynh, Mohamed Reda Bouadjenek, Sunil Aryal, Imran Razzak, and Hakim Hacid. Visual question answering: from early developments to recent advances—a survey. *arXiv preprint arXiv:2501.03939*, 2025.

[47] Zhong-Qiu Zhao, Peng Zheng, Shou-tao Xu, and Xindong Wu. Object detection with deep learning: A review. *IEEE transactions on neural networks and learning systems*, 30(11):3212–3232, 2019.

[48] Grégoire Mialon, Roberto Dessì, Maria Lomeli, Christoforos Nalmpantis, Ramakanth Pasunuru, Roberta Raileanu, Baptiste Roziere, Timo Schick, Jane Dwivedi-Yu, Asli Celikyilmaz, Edouard Grave, Yann LeCun, and Thomas Scialom. Augmented language models: a survey. *Transactions on Machine Learning Research*, 2023. ISSN 2835-8856.

[49] Yuqi Zhu, Shuofei Qiao, Yixin Ou, Shumin Deng, Shiwei Lyu, Yue Shen, Lei Liang, Jinjie Gu, Huajun Chen, and Ningyu Zhang. KnowAgent: Knowledge-augmented planning for LLM-based agents. In *Findings of the Association for Computational Linguistics: NAACL 2025*, pages 3709–3732, 2025.

[50] Tu Vu, Mohit Iyyer, Xuezhi Wang, Noah Constant, Jerry Wei, Jason Wei, Chris Tar, Yun-Hsuan Sung, Denny Zhou, Quoc Le, and Thang Luong. FreshLLMs: Refreshing large language models with search engine augmentation. In *Findings of the Association for Computational Linguistics: ACL 2024*, pages 13697–13720, 2024.

[51] Xingxuan Li, Ruochen Zhao, Yew Ken Chia, Bosheng Ding, Shafiq Joty, Soujanya Poria, and Lidong Bing. Chain-of-knowledge: Grounding large language models via dynamic knowledge adapting over heterogeneous sources. In *Proceedings of the 12th International Conference on Learning Representations*, ICLR, 2024.

[52] Harsh Trivedi, Niranjan Balasubramanian, Tushar Khot, and Ashish Sabharwal. Interleaving retrieval with chain-of-thought reasoning for knowledge-intensive multi-step questions. In *Proceedings of the 61st Annual Meeting of the Association for Computational Linguistics*, ACL, pages 10014–10037, 2023.

[53] Shuofei Qiao, Honghao Gui, Chengfei Lv, Qianghuai Jia, Huajun Chen, and Ningyu Zhang. Making language models better tool learners with execution feedback. In *Proceedings of the 2024 Conference of the North American Chapter of the Association for Computational Linguistics: Human Language Technologies*, NNACL, pages 3550–3568, 2024.

[54] J S Wind. 1st place solution + code and official documentation. <https://www.kaggle.com/competitions/abstraction-and-reasoning-challenge/discussion/154597>, 2020. Accessed: 2025-03-22.

[55] Giacomo Camposampiero, Loic Houmar, Benjamin Estermann, Joël Mathys, and Roger Wattenhofer. Abstract visual reasoning enabled by language. *arXiv preprint arXiv:2306.04091*, 2023.

[56] Tan John Chong Min. An approach to solving the abstraction and reasoning corpus (arc) challenge. *arXiv preprint arXiv:2306.03553*, 2023.

[57] John Chong Min Tan and Mehul Motani. Llms as a system of multiple expert agents: An approach to solve the abstraction and reasoning corpus (arc) challenge. In *Proceedings of the 2024 IEEE Conference on Artificial Intelligence*, CAI, pages 782–787, 2024.

[58] Kiril Bikov, Mikel Bober-Irizar, and Soumya Banerjee. Reflection system for the abstraction and reasoning corpus. In *Proceedings of the 2nd AI4Research Workshop: Towards a Knowledge-grounded Scientific Research Lifecycle*, 2024.

[59] Daniel Franzen, Jan Disselhoff, and David Hartmann. The llm architect: Solving arc-agi is a matter of perspective. [https://github.com/da-fr/arc-prize-2024/blob/main/the\\_architects.pdf](https://github.com/da-fr/arc-prize-2024/blob/main/the_architects.pdf), 2024. Accessed: 2025-03-22.

[60] Michael Hodel. Addressing the abstraction and reasoning corpus via procedural example generation. *arXiv preprint arXiv:2404.07353*, 2024.

[61] Arseny Moskvichev, Victor Vikram Odouard, and Melanie Mitchell. The conceptarc benchmark: Evaluating understanding and generalization in the arc domain. *arXiv preprint arXiv:2305.07141*, 2023.

[62] Wen-Ding Li, Keya Hu, Carter Larsen, Yuqing Wu, Simon Alford, Caleb Woo, Spencer M. Dunn, Hao Tang, Wei-Long Zheng, Yewen Pu, and Kevin Ellis. Combining induction and transduction for abstract reasoning. In *Proceedings of the 13th International Conference on Learning Representations*, ICLR, 2025.

[63] Shraddha Barke, Emmanuel Anaya Gonzalez, Saketh Ram Kasibatla, Taylor Berg-Kirkpatrick, and Nadia Polikarpova. Hysynth: Context-free llm approximation for guiding program synthesis. In *Proceedings of the 38th Advances in Neural Information Processing Systems*, NeurIPS, pages 15612–15645, 2024.

## A Appendix

### A.1 Related Work

**Knowledge-Augmented LLMs.** Augmenting LLMs with external knowledge can improve reasoning capabilities and mitigate hallucination in text generation [48]. Previous studies achieve this by incorporating domain-specific knowledge, designed by human experts [49], retrieved via search engines [50], or extracted from Wikipedia documents [51]. Trivedi et al. [52] demonstrated that interleaving knowledge augmentation within reasoning steps further reduces model hallucination, resulting in more accurate multi-step reasoning. Additionally, augmenting LLMs with execution feedback improves performance on both question answering [53] and program synthesis tasks [10, 17, 19].

**Search in DSL.** An abstract, expressive, and compositional representation of core knowledge priors is essential for solving ARC tasks [5]. Previous studies have manually encoded these priors into domain-specific languages (DSLs) with lifted relational representations [9, 10, 54]. Various program synthesis methods have been proposed to search for valid solution programs within their DSLs, including DAG-based search [54], graph-based constraint-guided search [9], and generalized planning [10]. Hand-crafted DSLs encode core knowledge priors with high precision and interpretability, enabling structured program synthesis. However, comprehensive DSLs induce large search spaces, limiting synthesis efficiency.

**LLMs for ARC.** Recent studies have explored using LLMs as ARC solvers to directly generate test output matrices and have prompted LLMs with different problem descriptions to improve output accuracy. Camposampiero et al. [55] employed LLMs to generate output grids from textual task descriptions, derived from a vision module which is designed to capture human-like visual priors. Min [56] prompted LLMs with the raw 2D matrices of each task, along with transformation and abstraction examples. Xu et al. [34] demonstrated that object representations derived from predefined abstractions can improve LLM performance on ARC tasks. Recent advances in code generation by LLMs [18, 17, 14] highlight their potential to replace search-based program synthesis, addressing efficiency limitations. Tan and Motani [57] evaluated LLM performance on the ARC benchmark by generating Python program solutions. Additionally, Wang et al. [36] approached ARC as an inductive reasoning problem and introduced hypothesis search, where program solutions are generated by selecting LLM-generated hypotheses encoded as functions.

**Training-Based Methods.** To further improve LLM performance, Bikov et al. [58] fine-tuned LLMs on augmented ARC tasks using standard techniques such as rotation, flipping, and permutation. Beyond these methods, Franzen et al. [59] fine-tuned LLMs on large-scale synthetic ARC tasks [60] and ARC-related datasets such as Concept-ARC [61] and ARC-Heavy [62], achieving a state-of-the-art 56% accuracy on the private evaluation set of 200 tasks. Instead of fine-tuning LLMs, Barke et al. [63] trained a probabilistic context-free grammar (PCFG) using LLM-generated plausible solutions to learn weighted functions. This enables the synthesizer to efficiently generate final program solutions. However, this approach requires a dedicated synthesizer for each DSL, limiting its generalization.

When leveraging LLMs as ARC solvers, existing studies tend to emphasize accuracy on partial training set problems and overlook the core principle of ARC, where solutions should be constructed using core knowledge priors [5]. LLMs still lack these priors, such as objectness, as evidenced by RSPC-generated solutions. Although fine-tuning approaches have achieved state-of-the-art performance, their failure to incorporate core knowledge priors remains a fundamental limitation. KAAR addresses this gap by progressively augmenting LLMs with structured core knowledge priors introduced by GPAR, along with exclusive implementations of goal-directedness priors. It interleaves augmentation within the reasoning process by applying an advanced LLM-based program synthesis solver tailored to the ARC benchmark after augmenting priors at each level. KAAR achieves strong performance, 32.5% test accuracy on the full evaluation set of 400 problems using GPT-o3-mini, demonstrates substantial generalization, and produces solutions aligned with core knowledge priors.

### A.2 Core Knowledge Priors in KAAR

KAAR incorporates abstractions to enable objectness priors; component attributes, relations, and statistical analysis of component attributes to encode geometry, topology, numbers, and counting priors; and predefined actions to support goal-directedness priors. Table 5 presents all abstractions



Figure 10: ARC problem 0520fde7

used in KAAR, organized by their prioritization. KAAR incorporates fundamental abstractions, such as 4-connected and 8-connected components, from GPAR, and extends them with additional abstractions unique to KAAR, highlighted in red. Table 6 introduces geometry, topology, numbers, and counting priors, and ten predefined transformations used in KAAR. For each action, KAAR augments the LLM with its corresponding schema to resolve implementation details. The actions and their schemas are detailed in Table 7. Most actions can be specified within three steps, keeping them tractable for LLMs.

### A.3 Restrictions in KAAR

For certain abstractions, some priors are either inapplicable or exclusive. The specific priors assigned to some abstractions are detailed in Table 8. For the *whole image* abstraction, few priors apply as only a single component is present. In contrast, the *4/8-connected-multi-color-non-background* abstractions retain most priors. The highlighted priors that capture per-component color diversity are used exclusively for *4/8-connected-multi-color-non-background* abstractions, while priors tailored to a single-color component, such as *components with same color*, *components with most frequent color*, and *components with least frequent color*, are excluded. For the *middle-vertical* and *middle-horizontal* abstractions, where the image is evenly divided into two components, flipping and movement actions are enabled to facilitate reasoning over overlapping components. For instance, in the problem shown in Figure 10, the solution involves splitting the image along a middle-vertical grid line and moving one component to overlap the other. In the resulting component, a pixel is colored red if the overlapping pixels in both components are blue; otherwise, it is colored black.

### A.4 Parameter Settings

KAAR operates on all LLMs through API access with the full conversational history. For proprietary models, GPT-03-mini and Gemini-2.0 Flash-Thinking (Gemini-2.0), we use default parameter settings. For open-source models, DeepSeek-R1-Distill-Llama-70B (DeepSeek-R1-70B) and QwQ-32B, we set temperature to 0.6, top-p to 0.95, and top-k to 40 to reduce repetitive outputs and filter rare tokens while preserving generation diversity. We conduct experiments on a virtual machine with 4 NVIDIA A100 80GB GPUs.

### A.5 KAAR

Algorithm 1 presents the pseudocode of KAAR. For each abstraction, KAAR incrementally augments the LLM with core knowledge priors, structured into three dependency-aware levels: beginning with objectness (Line 5), followed by geometry and topology (Lines 10 and 12), numbers and counting (Line 14), and concluding with goal-directedness priors (Line 18). We note that KAAR encodes geometry and topology priors through component attributes (Line 9) and relations (Line 11). The full set of priors is detailed in Tables 5, 6, and 7. After augmenting each level of priors, KAAR invokes the solver backbone (RSPC) at Lines 6, 15, and 19 to generate code solutions guided by text-based plans, allowing up to 4 iterations (Lines 25–37). In each iteration, the solver backbone first validates the generated code on the training instances  $I_r$ ; if successful, it then evaluates the solution on the test instances  $I_t$ . The solver backbone returns `solve` if the generated solution successfully solves  $I_t$  after passing  $I_r$ ; `pass` if only  $I_r$  is solved; or continues to the next iteration if the solution fails on  $I_r$ . If the solver backbone fails to solve  $I_r$  within the allotted 4 iterations at Lines 6 and 15, KAAR augments the next level of priors. KAAR proceeds to the next abstraction when the solver backbone fails to solve  $I_r$  at Line 19, after the 4-iteration limit. KAAR terminates abstraction iteration upon receiving either `pass` or `solve` from the solver backbone and reports accuracy on  $I_r$ ,  $I_t$ , and  $I_r \& I_t$  accordingly. If no abstraction fully solves  $I_r$ , KAAR records the final code solution for each abstraction (Line 22), selects the one that passes the most training instances (Line 23), and evaluates it on  $I_t$  to determine additional accuracy gains (Line 24).

---

**Algorithm 1:** KAAR

---

```
1 Input :LLM  $\mathcal{M}$ ; ARC problem  $\mathcal{P} = (I_r, I_t)$ ; description  $Q = (I_r, \{i^i \mid (i^i, i^o) \in I_t\})$ ;  
2 abstraction list  $\mathcal{A}$ ; max iterations  $t = 4$   
3 Function KnowledgeAugmentation ( $\mathcal{M}, Q, \mathcal{P}, \mathcal{A}, t$ ):  
4   solutionList  $\leftarrow \emptyset$ ;  
5   foreach abstraction  $abs$  in  $\mathcal{A}$  do  
6     objectnessPriors  $\leftarrow$  GenerateObjectnessPriors( $Q, abs$ );  
7     AugmentKnowledge( $\mathcal{M}$ , objectnessPriors);  
8     result, code, passedCount  $\leftarrow$  SolverBackbone ( $\mathcal{M}, \mathcal{P}, Q, t$ );  
9     if  $result \neq \text{failure}$  then  
10       return result  
11     attributePriors  $\leftarrow$  GenerateAttributePriors( $Q, abs$ );  
12     AugmentKnowledge( $\mathcal{M}$ , attributePriors);  
13     relationPriors  $\leftarrow$  GenerateRelationPriors( $Q, abs$ );  
14     AugmentKnowledge( $\mathcal{M}$ , relationPriors);  
15     numberPriors  $\leftarrow$  GenerateNumbersCountingPriors( $Q, abs$ );  
16     AugmentKnowledge( $\mathcal{M}$ , numberPriors);  
17     result, code, passedCount  $\leftarrow$  SolverBackbone ( $\mathcal{M}, \mathcal{P}, Q, t$ );  
18     if  $result \neq \text{failure}$  then  
19       return result  
20     AugmentGoalPriors  $\leftarrow$  ( $\mathcal{M}, Q, abs$ );  
21     result, code, passedCount  $\leftarrow$  SolverBackbone ( $\mathcal{M}, \mathcal{P}, Q, t$ );  
22     if  $result \neq \text{failure}$  then  
23       return result  
24     solutionList.append((code, passedCount));  
25   bestCode  $\leftarrow$  SelectMostPassed(solutionList);  
26   return EvaluateOnTest(bestCode,  $I_t$ );  
27 Function SolverBackbone ( $\mathcal{M}, \mathcal{P}, Q, t$ ):  
28   i  $\leftarrow 0$ ;  
29   while  $i < t$  do  
30     plan  $\leftarrow \mathcal{M}.\text{generatePlan}(Q)$ ;  
31     code  $\leftarrow \mathcal{M}.\text{generateCode}(Q, \text{plan})$ ;  
32     passedCount  $\leftarrow$  EvaluateOnTrain(code,  $I_r$ );  
33     if  $passedCount == |I_r|$  then  
34       if EvaluateOnTest(code,  $I_t$ ) then  
35         return solve, code, passedCount;  
36     i  $\leftarrow i + 1$ ;  
37   return failure, code, passedCount;
```

---

KAAR generates priors offline using image processing algorithms introduced in GPAR at Lines 4, 9, 11 and 13. In contrast, KAAR enables goal-directedness priors at Line 18 by prompting the LLM to select the most suitable actions and identify their implementation details, as described in Table 7. KAAR iterates over abstractions from simpler to more complex, following the order specified in Table 5. We note that the highest-priority abstraction is *no abstraction*, where KAAR degrades to the solver backbone (RSPC) as no priors are applied.

## A.6 Ablation Study

Table 3 reports the accuracy decrease resulting from removing incremental knowledge augmentation and stage-wise reasoning in KAAR, denoted as KAAR\*. Unlike KAAR, which invokes the solver backbone (RSPC) after augmenting each level of priors to enable stage-wise reasoning, KAAR\* uses RSPC to solve the problem within 12 iterations after augmenting all priors at once. We evaluate

		KAAR	KAAR*	$\Delta$
Gemini-2.0	$I_r$	25.75	23.00	-2.75
	$I_t$	21.75	19.00	-2.75
	$I_r \& I_t$	20.50	18.00	-2.50
QwQ-32B	$I_r$	22.25	18.50	-3.75
	$I_t$	21.00	17.75	-3.25
	$I_r \& I_t$	19.25	16.25	-3.00
DeepSeek-R1-70B	$I_r$	12.25	9.00	-3.25
	$I_t$	12.75	9.00	-3.75
	$I_r \& I_t$	11.50	8.50	-3.00

Table 3: Accuracy on  $I_r$ ,  $I_t$ , and  $I_r \& I_t$  for KAAR and KAAR\* across three LLMs. KAAR\* invokes the solver backbone (RSPC) only after all knowledge priors are augmented.  $\Delta$  denotes the performance drop relative to KAAR. All values are reported as percentages.

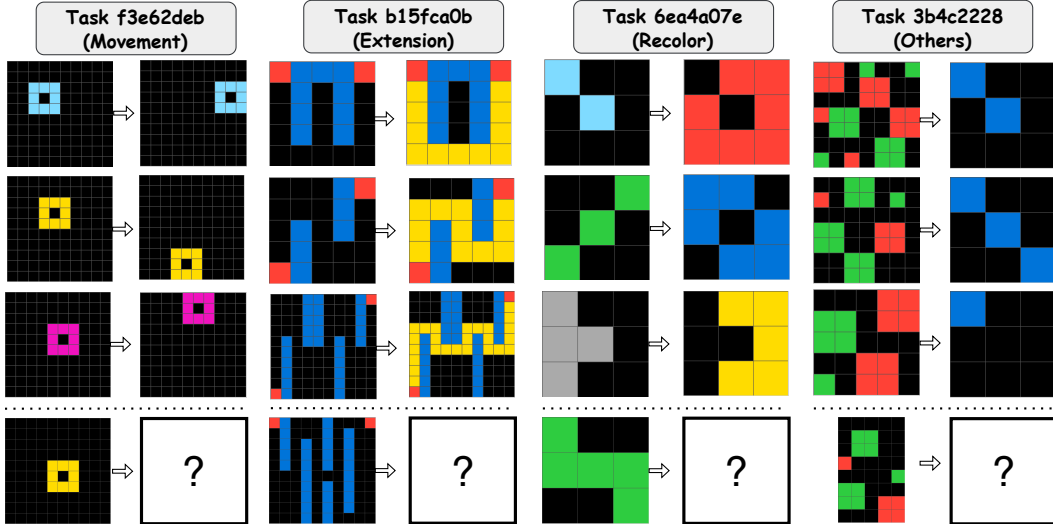


Figure 11: Example ARC tasks for *movement*, *extension*, *recolor*, and *others* categories.

KAAR\* using the same reasoning-oriented LLMs as in Tables 1 and 2, excluding GPT-o3-mini due to its computational cost. KAAR\* shows decreased accuracy on all metrics,  $I_r$ ,  $I_t$ , and  $I_r \& I_t$ , for all evaluated LLMs. These results underscore the effectiveness of progressive augmentation and stage-wise reasoning. Presenting all knowledge priors simultaneously introduces superfluous information, which may obscure viable solutions and impair the LLM reasoning accuracy. We note that we construct the ontology of core knowledge priors based on their dependencies, thereby establishing a fixed augmentation order.

#### A.7 Example Tasks by Category in the ARC Evaluation Set

ARC comprises 1000 unique tasks, with 400 allocated to the training set and 600 to the evaluation set. The evaluation set is further divided into a public subset (400 tasks) and a private subset (200 tasks). Figure 11 illustrates example ARC tasks for the *movement*, *extension*, *recolor*, and *others* categories in the public evaluation set. In the *movement* example, components are shifted to the image boundary in directions determined by their colors. The *extension* example is more complex, requiring LLMs to find the shortest path between two red pixels while avoiding obstacles, which presents challenges for current reasoning-oriented models. Additionally, reliance on pixel-level recognition weakens the effectiveness of KAAR, which is designed to facilitate component identification. The *recolor* example involves changing non-black components to black and updating black components based on original non-black colors. The *others* example requires generating a blue diagonal line whose length depends on the number of 4-connected components in the input image that are green and have a size

	Knowledge Augmentation	Solver Backbone (RSPC)
GPT-o3-mini	66K	106K
Gemini	58K	110K
QwQ-32B	79K	427K
DeepSeek-R1-70B	66K	252K

Table 4: Average token cost for knowledge augmentation and solver backbone (RSPC) in KAAR across four evaluated LLMs. K is  $10^3$ .

greater than one. The combination of numerical reasoning and structural pattern generation makes this task difficult to classify within the other three categories.

### A.8 Cost Analysis

Table 4 reports the average token cost, including both prompts and LLM responses, for knowledge augmentation and the solver backbone (RSPC), when using KAAR as the ARC solver. For each ARC task, we consider the abstraction whose solution solves  $I_t$ ; if none succeed, the one that passes  $I_r$ ; otherwise, the abstraction with the lowest token usage is selected. Except for goal-directedness priors, all core knowledge priors in KAAR are generated offline using image processing algorithms from GPAR, resulting in comparable augmentation costs across all evaluated models. In contrast, token usage by the solver backbone varies substantially due to differences in the LLMs’ abstract reasoning and generalization capabilities. GPT-o3-mini solves most tasks efficiently, with the lowest token consumption by the solver backbone, where tokens used for knowledge augmentation account for approximately 62% of the solver backbone’s token usage. However, the solver backbone consumes more tokens with QwQ-32B, as QwQ-32B consistently generates longer reasoning traces. In this case, tokens used for knowledge augmentation constitute only 19% of the solver backbone’s token usage. Figure 14 illustrates the average token cost for augmenting priors at each level in KAAR.

### A.9 Generalization

Figures 15 and 16 illustrate two ARC problems, *695367ec* and *b1fc8b8e*, where both RSPC and KAAR successfully solve the training instances  $I_r$  but fail on the test instances  $I_t$  when using GPT-o3-mini. For problem *695367ec*, the correct solution involves generating a fixed  $15 \times 15$  output image by repeatedly copying the input image, changing its color to black, and adding internal horizontal and vertical lines colored with the original input image’s color. However, the RSPC-generated code applies a distinct rule to each input image size without considering generalization. For problem *b1fc8b8e*, the solution requires accurate object recognition despite component contact, and correctly placing each component into one of the four corners. However, RSPC fails to recognize objectness, and its solution deviates from human intuition, being overfitted to  $I_r$ . For problems *695367ec* and *b1fc8b8e*, KAAR exhibits the same limitations, although it adopts abstractions to enable objectness. KAAR begins with the simplest abstraction, *no abstraction*, where KAAR degrades to RSPC. As a result, it generates the same solution as RSPC and terminates without attempting other abstractions, since the solution already solves  $I_r$  and is then evaluated on  $I_t$ , resulting in overfitting.

### A.10 Problem Coverage across ARC Solvers

We report the relative problem coverage across nine ARC solvers based on successful test instance solutions using GPT-o3-mini (Figure 17), Gemini-2.0 (Figure 18), QwQ-32B (Figure 19), and DeepSeek-R1-70B (Figure 20). Each cell  $(i, j)$  indicates the proportion of problems solved by the row solver that are also solved by the column solver. This is computed as  $\frac{|A_i \cap A_j|}{|A_i|}$ , where  $A_i$  and  $A_j$  are the sets of problems solved by the row and column solvers, respectively, following the same method used in Figure 5. Values close to 1 indicate that the column solver covers most problems solved by the row solver. GPT-o3-mini demonstrates the strongest overall coverage, with pairwise overlap consistently exceeding 0.55. Among all solvers, repeated sampling with standalone (*P*) and planning-aided code generation (*PC*) show the highest coverage, with column values consistently above 0.8 for GPT-o3-mini. This trend persists across Gemini-2.0, QwQ-32B, and DeepSeek-R1-70B.

Under these models, repeated sampling with planning-aided code generation exhibits better alignment than its standalone code generation counterpart, generally yielding higher coverage values. However, planning-aided code generation under the direct generation setting shows weaker alignment, with column values around 0.40 for Gemini-2.0 and 0.35 for QwQ-32B. Among the four evaluated LLMs, DeepSeek-R1-70B demonstrates the lowest average off-diagonal coverage (i.e.,  $i \neq j$ ) of 0.603, suggesting potential output instability and variation attributable to solver choice.

### A.11 Performance Analysis

Table 1 highlights performance variations across reasoning-oriented LLMs and ARC solvers with respect to both accuracy and generalization. Notably, the ARC solver, repeated sampling with standalone code generation, exhibits a substantial accuracy gap between  $I_r$  and  $I_r \& I_t$ , indicating limited generalization capability when using GPT-o3-mini and Gemini-2.0. In contrast, repeated sampling with planning-aided code generation demonstrates markedly improved generalization by preventing solutions from directly replicating the output matrices of training instances, as illustrated in Figure 21. This output copying, observed under repeated sampling with standalone code generation, accounts for approximately 24% and 95% of 83 and 101 overfitting problems with GPT-o3-mini and Gemini-2.0, respectively. When planning is incorporated, output copying is reduced to around 8% and 35% of 25 and 20 overfitting problems with GPT-o3-mini and Gemini-2.0, respectively. Additionally, the incorporation of planning facilitates accurate code generation. For example, in Figure 22, repeated sampling with planning-aided code generation produces a correct solution using GPT-o3-mini by replicating the input image horizontally or vertically based on the presence of a uniform row or column, as specified in the plan and implemented accordingly in code. In contrast, without planning assistance, standalone code generation produces incomplete logic, considering only whether the first column is uniform to determine the replication direction, which leads to failure on the test instance.

For the ARC benchmark, repeated sampling-based methods achieve higher accuracy on  $I_r$ ,  $I_t$ , and  $I_r \& I_t$  compared to refinement-based approaches when using GPT-o3-mini and Gemini-2.0. Figure 23 presents an ARC problem where repeated sampling with planning-aided code generation yields a correct solution, whereas its refinement variant fails to correct the initial erroneous code, and the flawed logic persists across subsequent refinements when using GPT-o3-mini. Previous studies have shown that refinement can benefit from control flow graph information [17] and verified plans [18], which assist LLMs in locating and correcting bugs. However, these methods typically incur substantial token consumption, making them difficult to scale affordably.

### A.12 Limitations

KAAR improves the performance of reasoning-oriented LLMs on ARC tasks by progressively prompting with core knowledge priors. Although this inevitably increases token usage, the trade-off can be justified, as the exploration of LLM generalization remains in its early stages. KAAR integrates diverse abstraction methods to enable objectness and iteratively applies abstractions in order of increasing complexity. In contrast, humans typically infer appropriate abstractions directly from training instances, rather than leveraging exhaustive search. To address this, we prompt different LLMs with raw 2D matrices of each ARC problem to select one or three relevant abstractions, but the results are unsatisfactory. As previously discussed, accurate abstraction inference often depends on validation through viable solutions, thereby shifting the challenge back to solution generation. Additionally, KAAR augments core knowledge priors through prompting but lacks mechanisms to enforce LLM adherence to these priors during reasoning. While the KAAR-generated solutions generally conform to core knowledge priors, the intermediate reasoning processes may deviate from the intended patterns. Future work could explore fine-tuning or reinforcement learning to better align model behavior with the desired reasoning patterns.

Abstractions	Definitions
<i>No Abstraction</i>	-
<i>Whole Image</i>	We consider the whole image as a component.
<i>Middle-Vertical</i>	We vertically split the image into two equal parts, treating each as a distinct component.
<i>Middle-Horizontal</i>	We horizontally split the image into two equal parts, treating each as a distinct component.
<i>Multi-Lines</i>	We use rows or columns with a uniform color to divide the input image into multiple components.
<i>4-Connected</i> <sup>*</sup>	We consider the 4-adjacent pixels of the same color as a component.
<i>4-Connected-Non-Background</i> <sup>*</sup>	We consider the 4-adjacent pixels of the same color as a component, excluding components with the background color.
<i>4-Connected-Non-Background-Edge</i> <sup>*</sup>	We consider the 4-adjacent pixels of the same color as a component, containing components with the background color when they are not attached to the edges of the image.
<i>4-Connected-Multi-Color-Non-Background</i> <sup>*</sup>	We consider 4-adjacent pixels as a component, which may contain different colors, while excluding components with the background color.
<i>4-Connected-Bounding-Box</i> <sup>*</sup>	We consider 4-adjacent pixels of the same color, and treat all pixels within their bounding box as a component, which may include different colors.
<i>4-Connected-With-Black</i> <sup>*</sup>	We consider the 4-adjacent pixels of black color, represented by the value 0, as a component, excluding components with other colors.
<i>Same-Color</i>	We consider pixels of the same color as a component, excluding components with the background color.

Table 5: Abstractions in KAAR. The superscript “\*” denotes that the 8-connected version is considered. The background color is black if black exists; otherwise, it is the most frequent color in the image. We present abstractions according to their prioritization in KAAR, where the order is given by the table from top to bottom, and making 8-connected abstraction to follow that of the corresponding 4-connected abstraction at the end of the sequence. Abstractions highlighted in red are exclusive to KAAR.

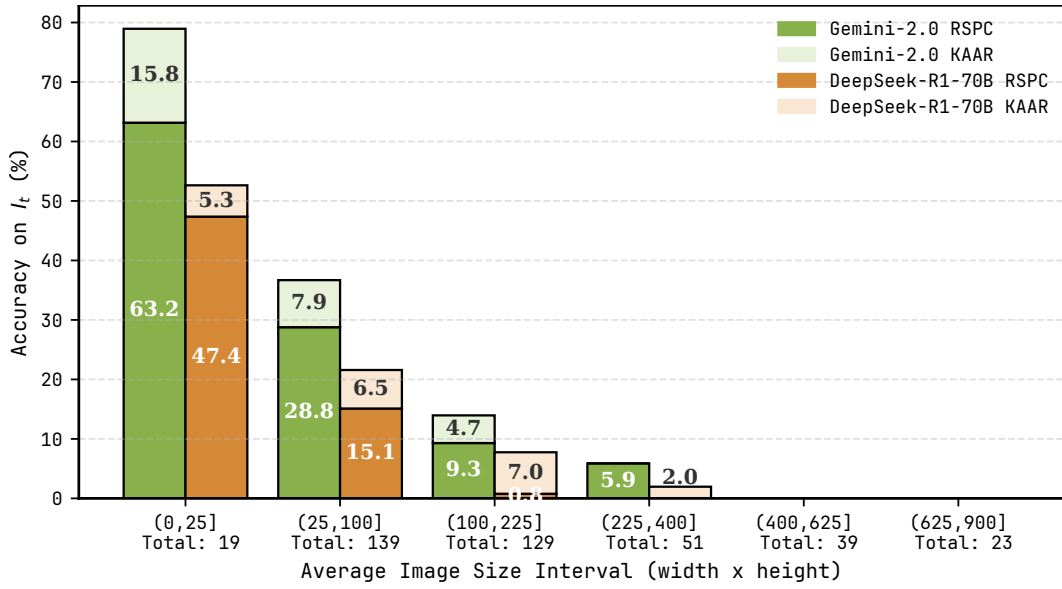


Figure 12: Accuracy on test instances  $I_t$  for RSPC and KAAR across average image size intervals, evaluated with Gemini-2.0 and DeepSeek-R1-70B.

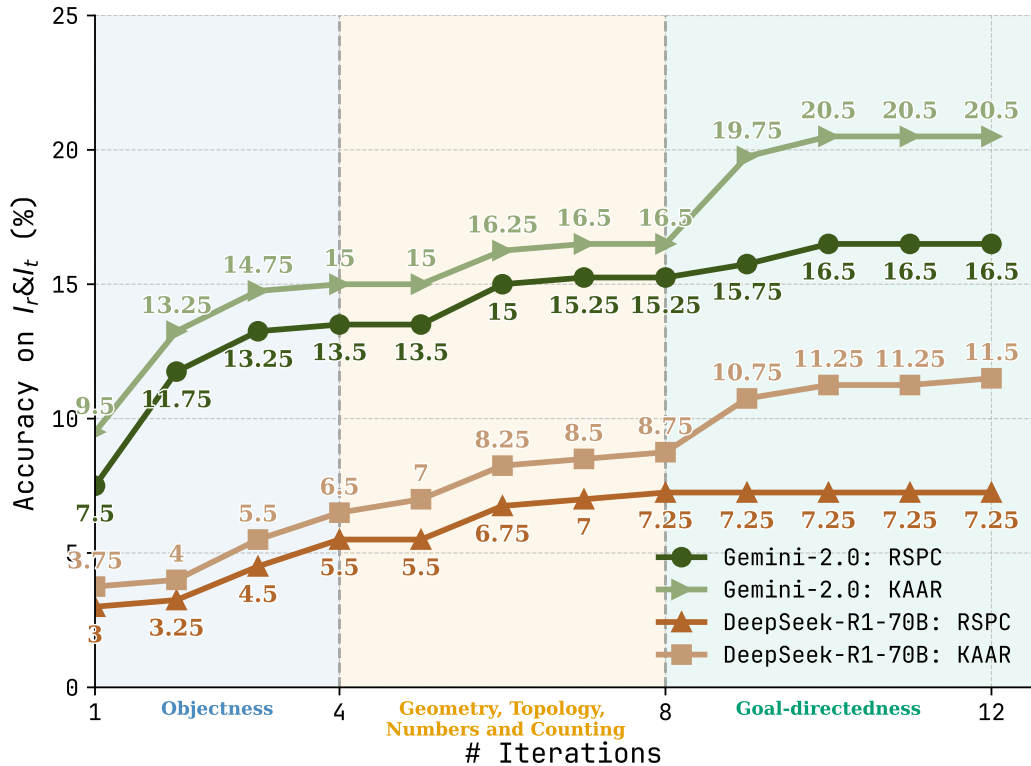


Figure 13: Variance in accuracy on  $I_r$  &  $I_t$  with increasing iterations for RSPC and KAAR using Gemini-2.0 and DeepSeek-R1-70B.

Classifications	Priors
<i>Geometry and Topology</i>	Size (Width and Height); Color; Shape (One Pixel; Horizontal Line; Vertical Line; Diagonal Line; Square; Rectangle; Cross; Irregular Shape); Symmetry (Horizontal Symmetry; Vertical Symmetry; Diagonal Symmetry; Anti-Diagonal Symmetry; Central Symmetry); Bounding Box; Hole Count; Nearest Boundary; Different/Identical with Other Components; Touching; Inclusive; Spatial (Horizontally Aligned to the Right; Horizontally Aligned to the Left; Vertically Aligned Below; Vertically Aligned Above; Top-Left; Top-Right; Bottom-Left; Bottom-Right; Same Position)
<i>Numbers and Counting</i>	Component Size Counting; Components with Same Size; Components with Most Frequent Size; Components with Least Frequent Size; Components with Maximum Size; Components with Minimum Size; Component Color Counting; Components with Same Color; Components with Same Number of Colors; Components with Most Frequent Color; Components with Least Frequent Color; Component with Most Distinct Colors; Component with Fewest Distinct Colors; Component Shape Counting; Components with Same Shape; Components with Most Frequent Shape; Components with Least Frequent Shape; Component Hole Number Counting; Components with Same Number of Holes; Components with Maximum Number of Holes; Components with Minimum Number of Holes; Component Symmetry Counting
<i>Goal-directedness</i>	Color Change (modifying component value); Movement (shifting component's position); Extension (expanding component's area); Completing (filling in missing parts of a component); Resizing (altering component size); Selecting (isolating a component); Copying (duplicating a component); Flipping (mirroring a component); Rotation (rotating a component); Cropping (cutting part of a component)

Table 6: KAAR priors classified into geometry and topology, numbers and counting, and goal-directedness. For goal-directedness, we incorporate ten predefined actions, with their corresponding action schemas detailed in Table 7.

Actions		Schemas (Implementation Details)					
<i>Color Change</i>		Targets Source and Target Colors					
<i>Movement</i>	Targets	Direction		Start and End Locations	Pattern	Order	Overlapping
<i>Extension</i>	Targets	Direction		Start and End Locations	Pattern	Order	Intersection
<i>Completing</i>	Targets	Pattern					
<i>Resizing</i>	Targets	Source and Target Sizes					
<i>Selecting</i>	Targets						
<i>Copying</i>	Targets	Locations		Overlapping			
<i>Flipping</i>	Targets	Flipping Axis		Overlapping			
<i>Rotation</i>	Targets	Degrees					
<i>Cropping</i>	Targets	Subsets					

Table 7: Actions in KAAR and their schemas (implementation details). Each action schema is presented according to its prompting order in KAAR (left to right). Some actions include a pattern schema that prompts the LLM to identify underlying logic rules, such as repeating every two steps in movement or extension, or completing based on three-color repetition. Targets denote the target components.

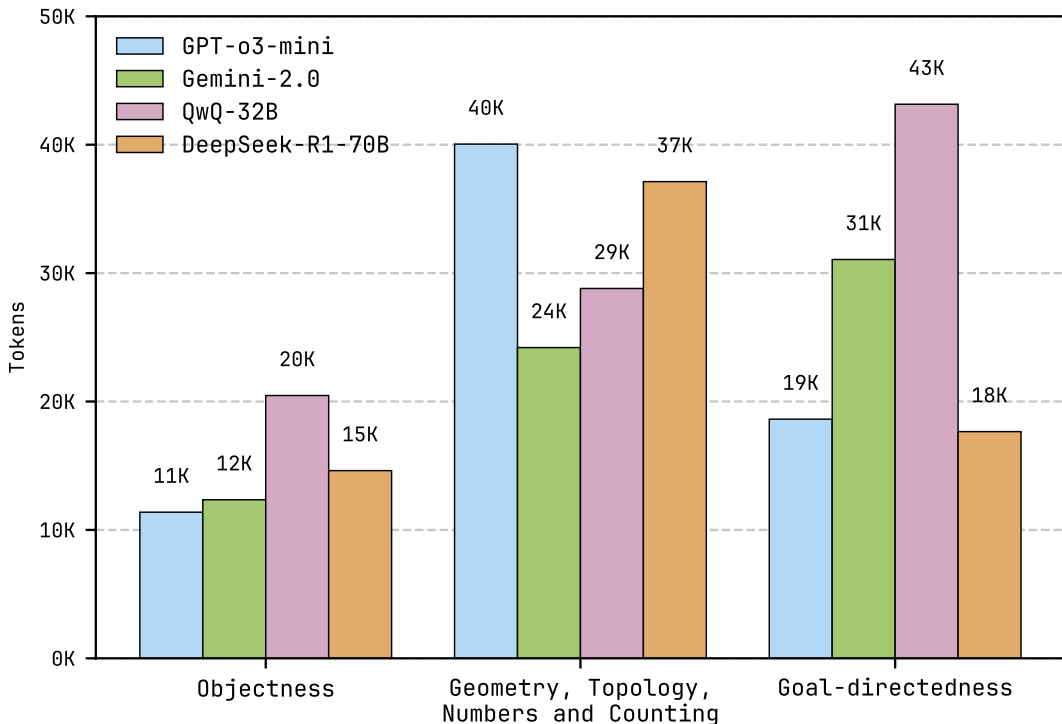


Figure 14: Average token cost for augmenting priors at each level across four LLMs. K is  $10^3$ .

Abstractions	Geometry and Topology	Numbers and Counting	Goal-directedness
<i>whole image</i>	Symmetry, Size	-	Flipping; Rotation; Extension; Completing, Cropping
<i>middle-vertical</i>	Size	-	Flipping; Movement
<i>middle-horizontal</i>	Size	-	Flipping; Movement
<i>multi-lines</i>	Size; Color; Shape; Symmetry; Bounding Box; Hole Count	ALL	ALL
<i>4-connected- multi-color-non- background<sup>*</sup></i>	ALL	... Component Color Counting; Components with Same Number of Colors; Component with Most Distinct Colors; Component with Fewest Distinct Colors ...	ALL

Table 8: Abstractions with their assigned knowledge priors. “–” denotes no priors, while “ALL” indicates all priors in the corresponding category, as defined in Table 6. The superscript “\*” indicates that the 8-connected version is also applicable. The highlighted priors apply exclusively to their corresponding abstractions. For the *4/8-connected-multi-color-non-background* abstractions, we present color-counting priors specific to multi-colored components, while all other non-color-counting priors follow those in Table 6.

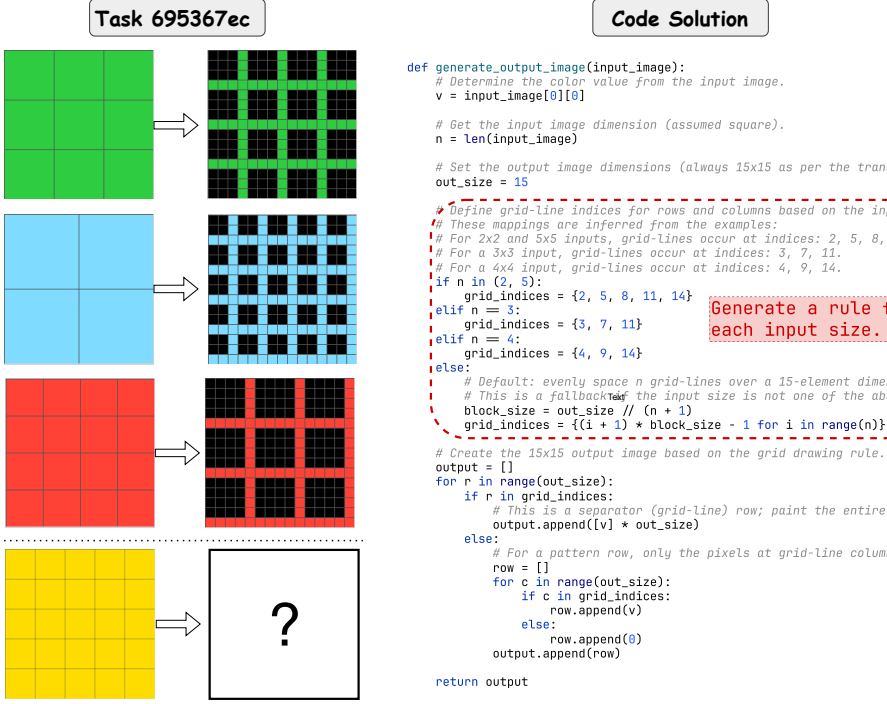


Figure 15: ARC problem 695367ec, where RSPC and KAAR generate the same code solution that passes the training instances but fails on the test instance using GPT-o3-mini.

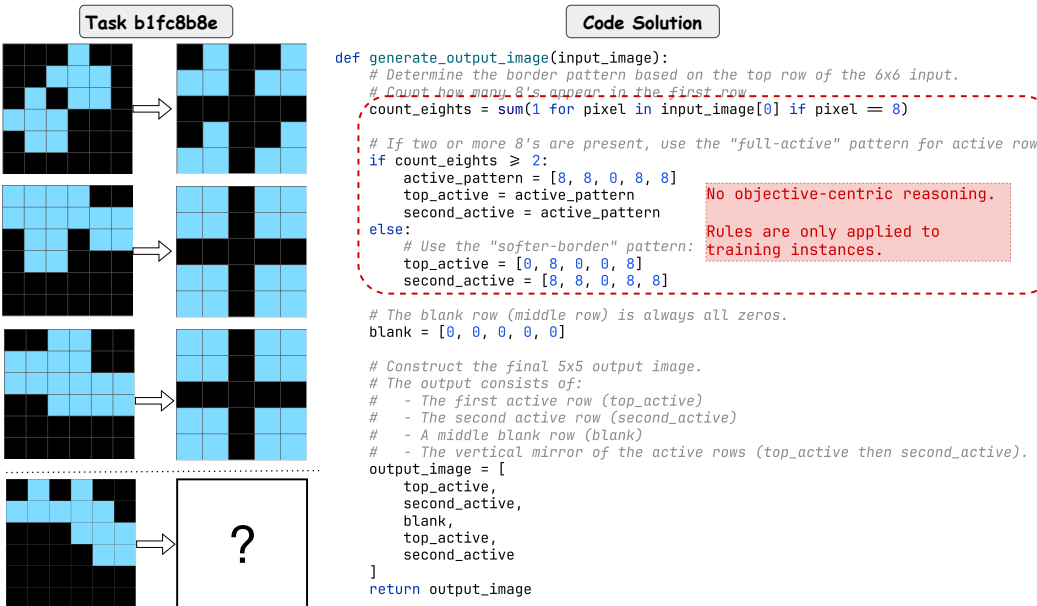


Figure 16: ARC problem b1fc8b8e, where RSPC and KAAR generate the same code solution that passes the training instances but fails on the test instance using GPT-o3-mini.

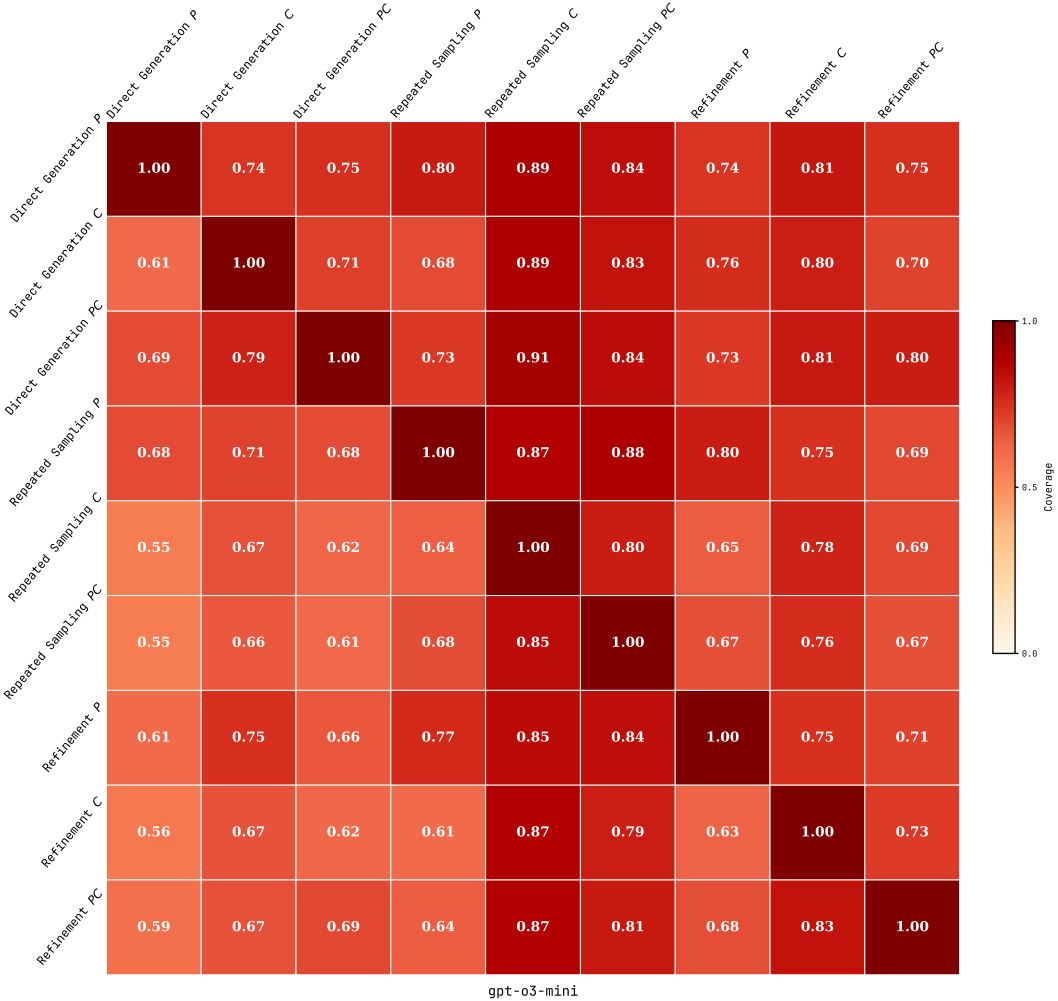


Figure 17: Asymmetric relative coverage matrix of nine ARC solvers using GPT-o3-mini, showing the proportion of problems whose test instances are solved by the row solver that are also solved by the column solver.  $P$  denotes the solution plan;  $C$  and  $PC$  refer to standalone and planning-aided code generation, respectively.

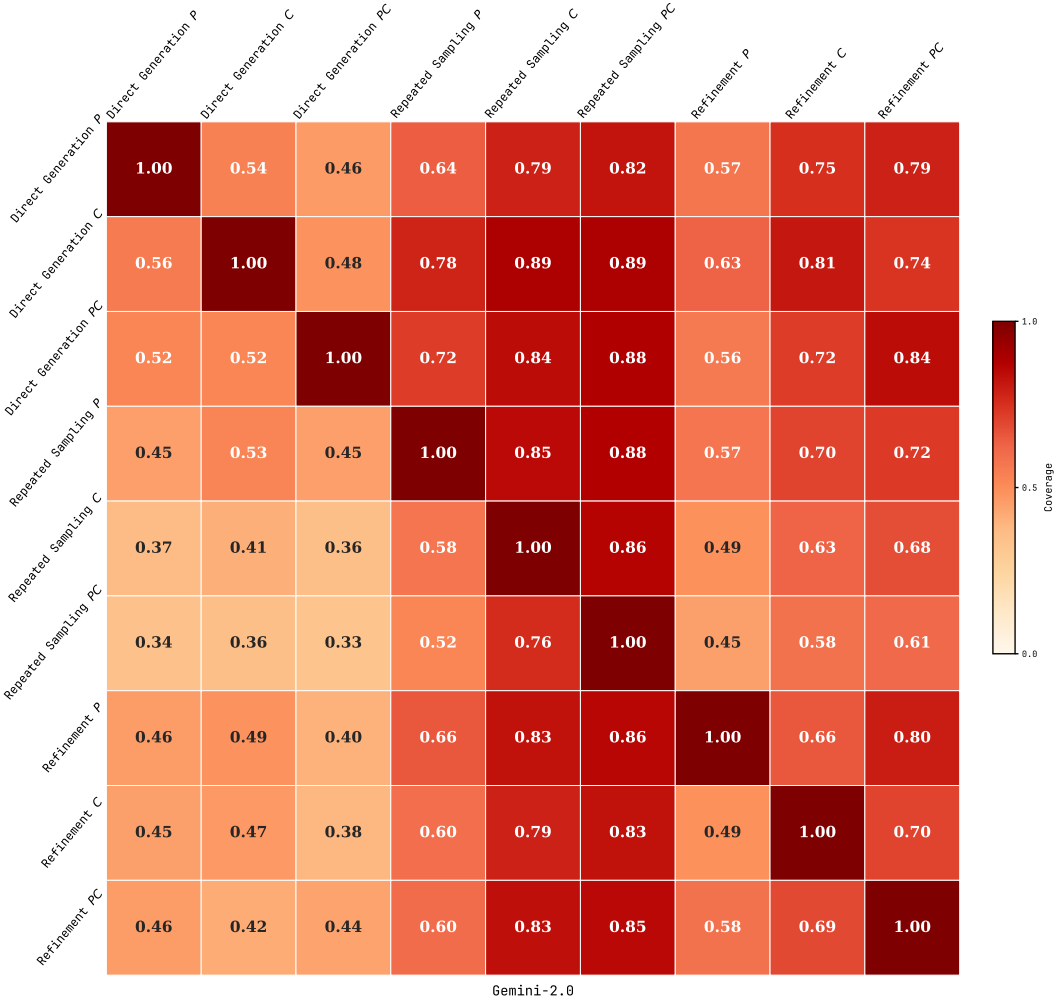


Figure 18: Asymmetric relative coverage matrix of nine ARC solvers using Gemini-2.0, showing the proportion of problems whose test instances are solved by the row solver that are also solved by the column solver.  $P$  denotes the solution plan;  $C$  and  $PC$  refer to standalone and planning-aided code generation, respectively.

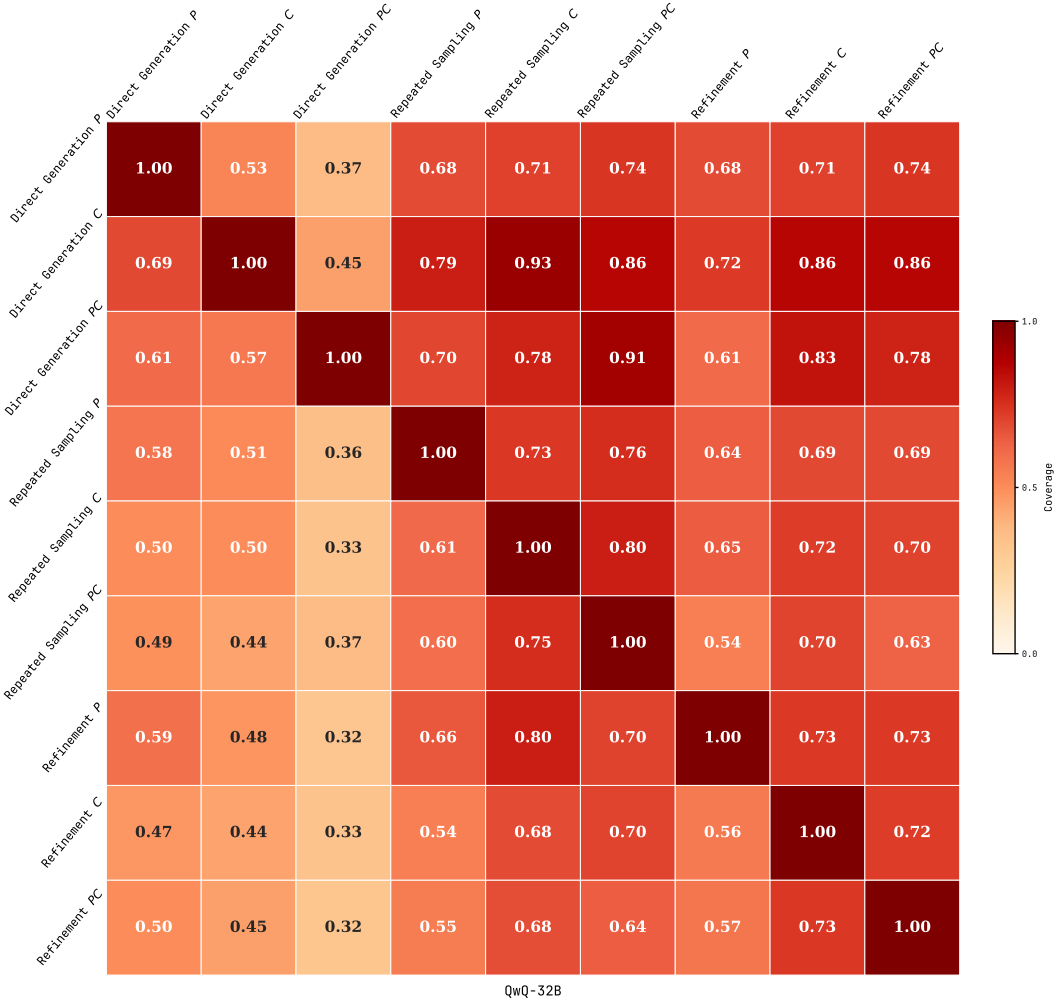


Figure 19: Asymmetric relative coverage matrix of nine ARC solvers using QwQ-32B, showing the proportion of problems whose test instances are solved by the row solver that are also solved by the column solver.  $P$  denotes the solution plan;  $C$  and  $PC$  refer to standalone and planning-aided code generation, respectively.

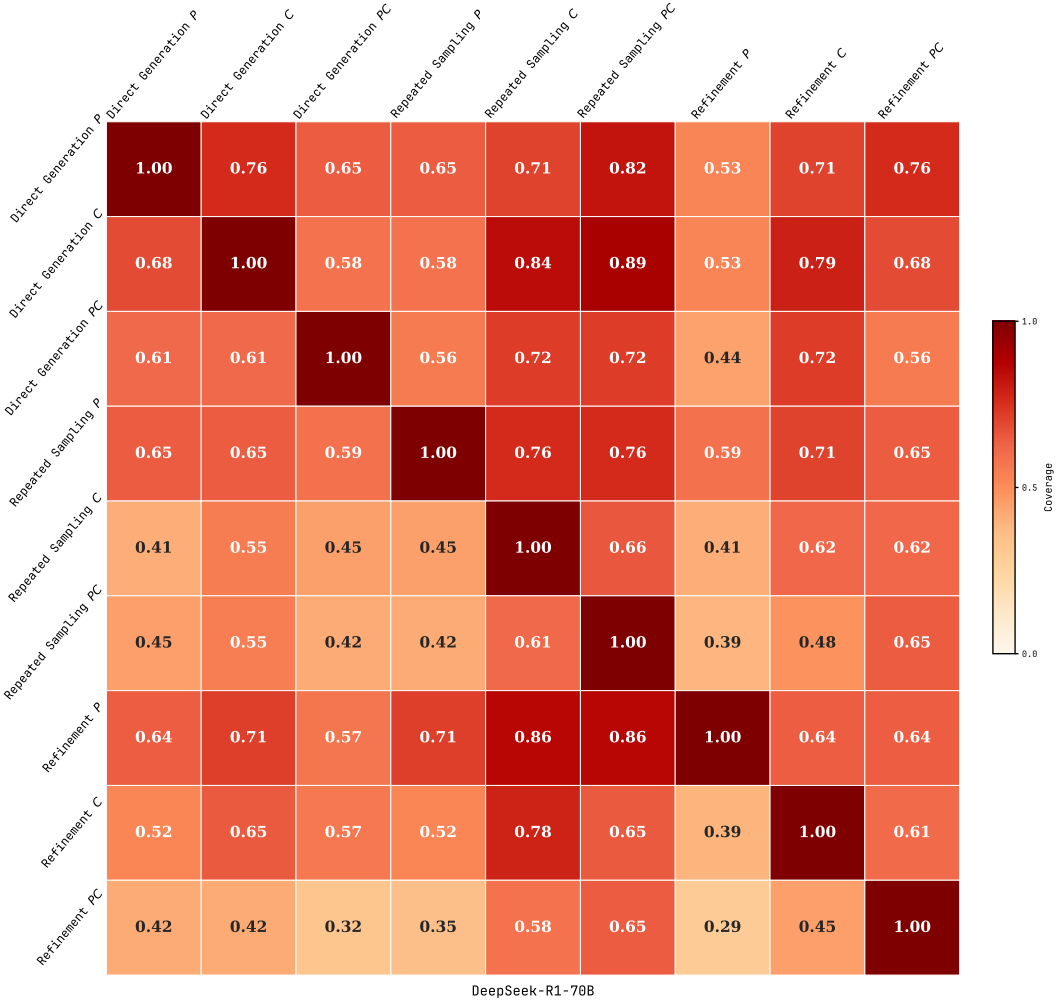
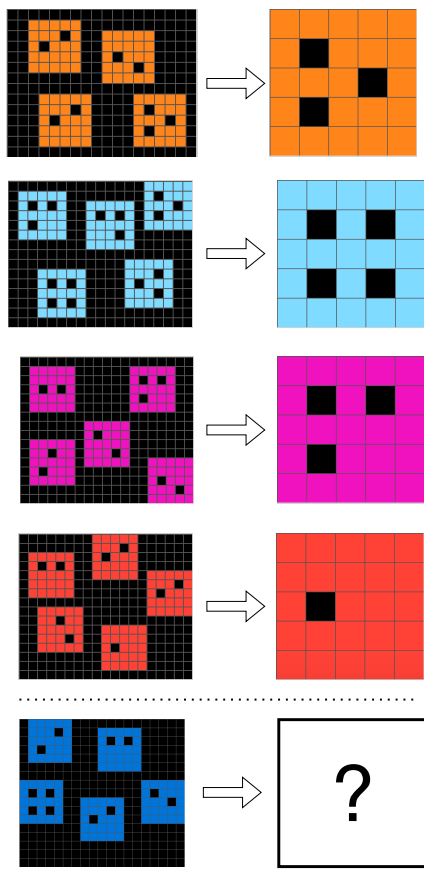


Figure 20: Asymmetric relative coverage matrix of nine ARC solvers using DeepSeek-R1-70B, showing the proportion of problems whose test instances are solved by the row solver that are also solved by the column solver.  $P$  denotes the solution plan;  $C$  and  $PC$  refer to standalone and planning-aided code generation, respectively.

**Task 358ba94e**



**Code Solution**

```

def generate_output_image(input_image):
    freq = {}
    for row in input_image:
        for pix in row:
            if pix != 0:
                freq[pix] = freq.get(pix, 0) + 1
    # If there is no non-zero pixel, return a 5x5 zero matrix.
    if not freq:
        return [[0, 0, 0, 0, 0] for _ in range(5)]
    # Determine the "digit" (nonzero value) that occurs most often.
    digit = max(freq, key=freq.get)

    # Return the fixed normalized 5x5 pattern corresponding to the detected digit.
    if digit == 7:
        return [
            [7, 7, 7, 7, 7],
            [7, 0, 7, 7, 7],
            [7, 7, 7, 0, 7],
            [7, 0, 7, 7, 7],
            [7, 7, 7, 7, 7]
        ]
    elif digit == 8:
        return [
            [8, 8, 8, 8, 8],
            [8, 0, 8, 0, 8],
            [8, 8, 8, 8, 8],
            [8, 0, 8, 0, 8],
            [8, 8, 8, 8, 8]
        ]
    elif digit == 6:
        return [
            [6, 6, 6, 6, 6],
            [6, 0, 6, 0, 6],
            [6, 6, 6, 6, 6],
            [6, 0, 6, 0, 6],
            [6, 6, 6, 6, 6]
        ]
    elif digit == 2:
        return [
            [2, 2, 2, 2, 2],
            [2, 0, 2, 2, 2],
            [2, 0, 2, 2, 2],
            [2, 2, 2, 2, 2],
            [2, 2, 2, 2, 2]
        ]
    elif digit == 1:
        # For the test image the drawn digit is 1.
        # We choose a pattern that follows a similar style to the others.
        return [
            [1, 1, 1, 1, 1],
            [1, 0, 1, 0, 1],
            [1, 1, 1, 1, 1],
            [1, 0, 1, 1, 1],
            [1, 1, 1, 1, 1]
        ]
    else:
        # For any other digit, simply fill a 5x5 matrix with that digit.
        return [[digit]*5 for _ in range(5)]

```

Copy the output matrices.

Figure 21: ARC problem 358ba94e, where repeated sampling with standalone code generation produces an incorrect solution using GPT-o3-mini.

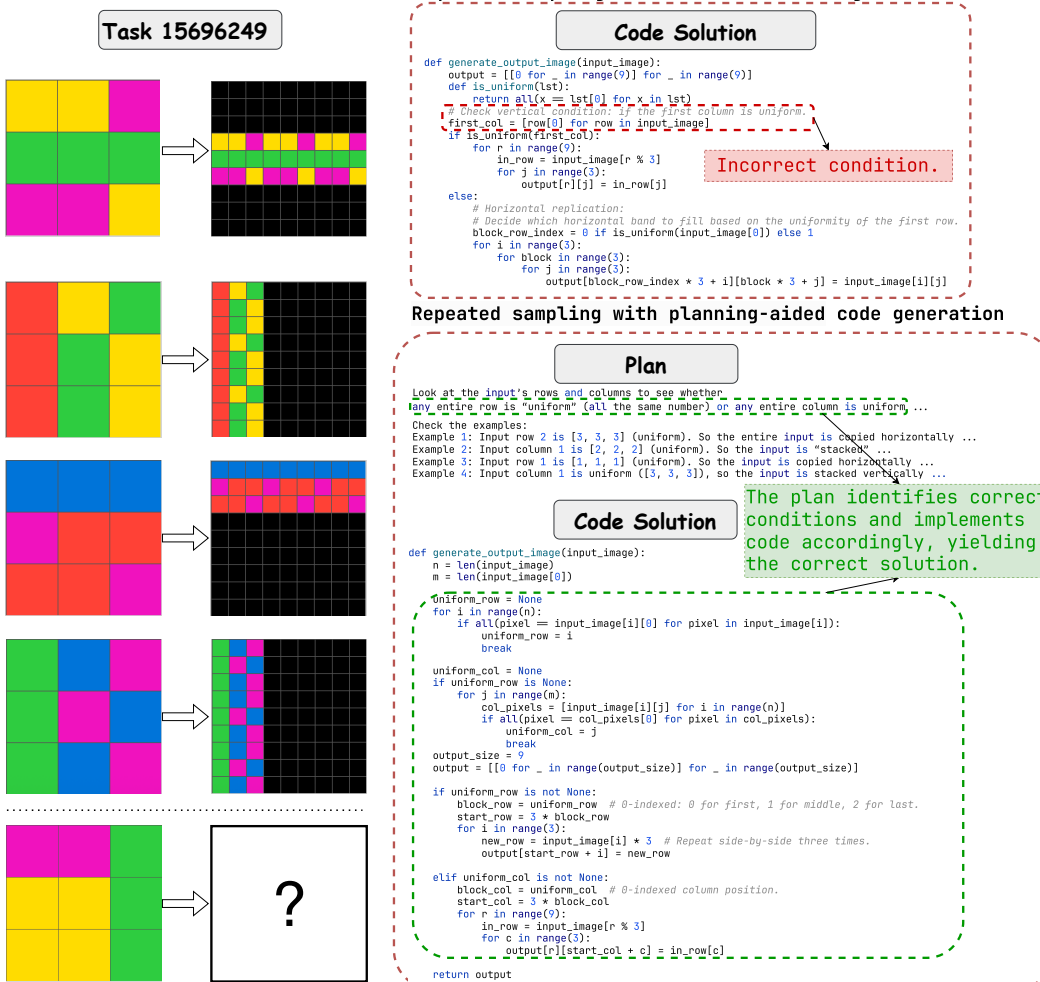
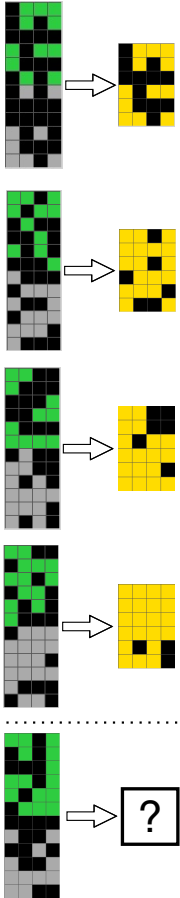


Figure 22: ARC problem 15696249, where repeated sampling with standalone code generation produces an incorrect solution, whereas repeated sampling with planning-aided code generation yields the correct solution using GPT-o3-mini.

### Refinement with planning-aided code generation

#### Task d19f7514



```

def generate_output_image(input_image):
    # Step 1: Discard the lower 6 rows to work only with the top 6 rows.
    cropped = [row[:] for row in input_image[:6]]

    # Step 2: Change every nonzero pixel to 4 (convert 3's or any nonzero values to 4).
    for r in range(len(cropped)):
        for c in range(len(cropped[r])):
            if cropped[r][c] != 0:
                cropped[r][c] = 4  Initial incorrect code

    # Step 3: Vertical propagation.
    # Process from the second row (index 1) downwards
    for r in range(1, len(cropped)):
        for c in range(len(cropped[r])):
            # If this pixel is 0 and the pixel immediately above is 4, fill it with 4.
            if cropped[r][c] == 0 and cropped[r-1][c] == 4:
                cropped[r][c] = 4

    return cropped

def generate_output_image(input_image):
    cropped = input_image[:6]
    rows = len(cropped)
    cols = len(cropped[0])  Incorrect code after refinements

    # Step 2. Build the base image: every nonzero becomes 4.
    base = [4 if pixel != 0 else 0 for pixel in row for row in cropped]

    # The output image starts with the first (top) row of the base.
    output = [base[0][:]]

    def is_active(row):
        return any(pixel != 0 for pixel in row)

    # Process each subsequent row.
    for r in range(1, rows):
        # Start with the base row.
        new_row = base[r][:]

        if is_active(cropped[r]):
            for c in range(cols):
                # Only consider blank cells that were not drawn originally.
                if new_row[c] == 0 and cropped[r][c] == 0:
                    # Propagate only if the cell directly above is 4.
                    if output[r-1][c] == 4:
                        # For a right border cell, propagate automatically.
                        if c == cols - 1:
                            new_row[c] = 4

                    else:
                        left_drawn = (c - 1 >= 0 and cropped[r][c - 1] != 0)
                        right_drawn = (c + 1 < cols and cropped[r][c + 1] != 0)
                        if left_drawn or right_drawn:
                            new_row[c] = 4

        output.append(new_row)
    return output

```

**Incorrect logic persists after refinements.**

### Repeated sampling with planning-aided code generation

#### Code Solution

```

def generate_output_image(input_image):
    # Split the input image into two halves
    num_rows = len(input_image)
    mid = num_rows // 2
    top_half = []
    bottom_half = []

    # Replace nonzero pixels with 4 in both halves
    for i in range(mid):
        top_half.append([4 if pixel != 0 else 0 for pixel in input_image[i]])
    for i in range(mid, num_rows):
        bottom_half.append([4 if pixel != 0 else 0 for pixel in input_image[i]])

    # Combine the corresponding rows of the top and bottom halves using pixelwise OR (nonzero becomes 4)
    output_image = []
    for i in range(mid):
        combined_row = []
        for j in range(len(top_half[i])):
            # If either pixel in the corresponding column is nonzero (i.e., equals 4), output 4; otherwise 0.
            if top_half[i][j] or bottom_half[i][j]:
                combined_row.append(4)
            else:
                combined_row.append(0)
        output_image.append(combined_row)

```

**Correct logic.**

Figure 23: ARC problem *d19f7514*, where repeated sampling with planning-aided code generation produces a correct solution, whereas its refinement variant fails to refine the initial erroneous code, and the incorrect logic persists across subsequent refinements when using GPT-o3-mini.

### A.13 Prompts for LLMs

We include all prompts used by KAAR and nine ARC solvers described in Section 3. We adopt a bash-like notation for input arguments within the prompts, such as  `${test_inputs}` denotes the test input 2D matrices. A brief description of the prompts used for each solver is provided below.

- **Direct generation with solution plan:** Prompt 1 describes how to generate the solution plan, and Prompt 2 uses the generated plan to produce the output images.
- **Direct generation with standalone code:** Prompt 3 describes how to generate the code to produce the output images.
- **Direct generation with planning-aided code:** It first generates a solution plan using Prompt 1, then uses Prompt 4 to produce code based on the generated plan.
- **Repeated sampling with solution plan:** It can be regarded as an iterative version of direct generation with solution plan, and thus also uses Prompts 1 and 2.
- **Repeated sampling with standalone code:** It can be regarded as an iterative version of direct generation with standalone code, and thus also uses Prompt 3.
- **Repeated sampling with planning-aided code:** It can be regarded as an iterative version of direct generation with planning-aided code, and thus also uses Prompts 1 and 4.
- **Refinement with solution plan:** Prompt 5 describes the process of refining the generated solution plan with the validation samples. It uses Prompts 1 and 2 to generate the initial plan and the result image.
- **Refinement with the standalone code:** Prompt 6 describes the process of refining the generated code with the validation samples. It uses Prompt 3 to produce the initial code solution.
- **Refinement with the planning-aided code:** Prompt 7 describes the process of refining the generated plan and code with the validation samples. It use Prompts 1 and 4 to generate the initial plan and produce the initial code guided by the plan, respectively.
- **KAAR:** Prompt 8 describes the augmentation of objectness priors. Prompts 9 and 10 introduce the augmentation of geometry and topology priors, encoded as component attributes and relations, respectively. Prompt 11 outlines the augmentation of numbers and counting priors. Prompts 12 and 13 describe action selection and target component identification in the process of augmenting goal-directedness priors. For prompts implementing each action's implementation details, please refer to our code.

Prompt 1: Direct generation with solution plan - solution plan generation.

```
===== System =====
You are an expert in analyzing grid-based image processing tasks. Your
objective is to derive a text transformation plan (not Python code) from
each given input-output image pair (both represented as 2D matrices), and
then apply this plan to generate output image(s), represented as a 2D
matrix, based on the given test input image(s) (2D matrix). Ensure that
the derived plan generalizes across different cases while preserving
consistency with the observed transformations.

===== User =====
The input data consists of a few pairs of input and output images, where
the left image in each pair represents the input, and the right image
represents the corresponding output. Each image can be represented as a 2
D matrix: ${matrix}

Please note that each number in the matrix corresponds to a pixel, and
its value represents the color.

Derive a text transformation plan (not Python code) that maps each given
input image (2D matrix) to its corresponding output image (2D matrix).
Ensure that the plan generalizes across different cases and the test
input image(s) (2D matrix) while maintaining consistency with the
observed transformations.
```

The test input image(s): \${test\_inputs}

Prompt 2: Direct generation with solution plan - output image(s) generation from the plan.

===== System =====  
You are an expert in analyzing grid-based image processing tasks. Your objective is to generate output image(s), represented as a 2D matrix, based on the given input images (2D matrix) and a derived text transformation plan.

===== User =====  
Please generate the output image(s) as a 2D matrix (not Python code) based on the given input image(s) (2D matrix) and the text transformation plan. Output only the test output image(s) in 2D matrix format (not Python code). For each test input image, start with [Start Output Image] and end with [End Output Image].

For example, if there is one test input image, the output image should be:

```
[Start Output Image]  
[[0,0,0], [0,0,0], [0,0,0]]  
[End Output Image]
```

If there are multiple (2) test input images, the the output images should be outputed as:

```
[Start Output Image]  
[[0,0,0], [0,0,0], [0,0,0]]  
[End Output Image]  
[Start Output Image]  
[[1,1,1], [1,1,1], [1,1,1]]  
[End Output Image]
```

The test input image(s): \${test\_inputs}

Prompt 3: Direct generation with standalone code.

===== System =====  
You are an expert in analyzing grid-based image processing tasks. Your goal is to generate Python code that produces output image(s), represented as a 2D matrix, based on the given input image(s) (2D matrix).

===== User =====  
The input data consists of a few pairs of input and output images, where the left image in each pair represents the input and the right image represents the corresponding output.

Each image can be represented as a 2D matrix: \${matrix}  
The test input image(s): \${test\_inputs}

Please note that each number in the matrix corresponds to a pixel, and its value represents the color.

Generate a Python script to map each input image (2D matrix) to the corresponding output image (2D matrix).

Ensure that the Python script generalizes across different cases and test input image(s) while maintaining consistency with the observed input-output image pairs.

Please output the Python program, starting with [Start Program] and ending with [End Program].

Include an assert statement with the function signature to verify that the generated output matches the expected result, starting with [Assert Statement].

Use placeholders like input\_image and output\_image for the variables representing the input and output images.

```

For example:
[Start Program]
def generate_output_image(input_image):
    rows = len(input_image)
    cols = len(input_image[0])

    def dfs(r, c):
        """Depth-first search to mark all 4-connected '1's to '2's."""
        if r < 0 or r >= rows or c < 0 or c >= cols or input_image[r][c]
        != 1:
            return
        # Change the current component from 1 to 2
        input_image[r][c] = 2
        # Explore neighbors (up, down, left, right)
        dfs(r - 1, c) # Up
        dfs(r + 1, c) # Down
        dfs(r, c - 1) # Left
        dfs(r, c + 1) # Right

    # Traverse the image to find all components with '1'
    for r in range(rows):
        for c in range(cols):
            if input_image[r][c] == 1:
                dfs(r, c)
    return input_image
[End Program]
[Assert Statement]
assert generate_output_image(input_image) == output_image

```

Please note, the assert statement should strictly follow the provided format, and the output image should be represented in list format!  
 Please note, the script should not include an if `__name__ == "__main__"`: block.

Prompt 4: Direct generation with planning-aided code - code generation based on the generated plan.

===== System =====  
 You are an expert in analyzing grid-based image processing tasks. Your goal is to generate Python code that produces output image(s) represented as a 2D matrix, based on the given input image(s) (2D matrix). This code should be generated using a text transformation plan inferred from a set of input-output image pairs (both represented as 2D matrices).

===== User =====  
 Generate a Python script based on your text transformation plan to map the input image (2D matrix) to the output image (2D matrix). Please output the Python program, starting with [Start Program] and ending with [End Program]. Include an assert statement with the function signature to verify that the generated output matches the expected result, starting with [Assert Statement]. Use placeholders like `input_image` and `output_image` for the variables representing the input and output images.

```

For example:
[Start Program]
def generate_output_image(input_image):
    rows = len(input_image)
    cols = len(input_image[0])

    def dfs(r, c):
        """Depth-first search to mark all 4-connected '1's to '2's."""
        if r < 0 or r >= rows or c < 0 or c >= cols or input_image[r][c]
        != 1:
            return
        # Change the current component from 1 to 2

```

```

        input_image[r][c] = 2
        # Explore neighbors (up, down, left, right)
        dfs(r - 1, c) # Up
        dfs(r + 1, c) # Down
        dfs(r, c - 1) # Left
        dfs(r, c + 1) # Right

    # Traverse the image to find all components with '1'
    for r in range(rows):
        for c in range(cols):
            if input_image[r][c] == 1:
                dfs(r, c)
    return input_image

[End Program]
[Assert Statement]
assert generate_output_image(input_image) == output_image

Please note, the assert statement should strictly follow the provided
format, and the output image should be represented in list format!
Please note, the script should not include an if __name__ == "__main__":
block.

```

Prompt 5: Refinement with solution plan - plan refinement.

```

=====
System =====
As an expert in analyzing grid-based image processing tasks, your
objective is to refine your solution plan based on the provided feedback.

=====
User =====
The problem description:
[start problem description]
The input data consists of a few pairs of input and output images, where
the left image in each pair represents the input, and the right image
represents the corresponding output. Each image can be represented as a 2
D matrix: ${matrix}
Please note that each number in the matrix corresponds to a pixel, and
its value represents the color.
[end problem description]

The INCORRECT text transformation plan fails to solve some example
training input and output pairs in the above problem!

[start incorrect transformation plan]
${plan}
[end incorrect transformation plan]

The incorrect output(s) generated by the incorrect plan:
[start incorrect output]
${incorrect_output}
[end incorrect output]

The generated correct output(s):
[start correct output]
${correct_output}
[end correct output]

Please analyze the incorrect reasoning step-by-step, and then generate
the revised correct transformation plan (text only), starting with [Start
Revised Transformation Plan] and ending with [End Revised Transformation
Plan]. Ensure that the revised transformation plan generalizes across
different cases and the test input image(s), while maintaining
consistency with the observed transformations.

```

Prompt 6: Refinement with standalone code - code refinement.

```
===== System =====
As an expert in analyzing grid-based image processing tasks, your
objective is to refine your program based on the provided feedback.

===== User =====
The problem description:
[start problem description]
The input data consists of a few pairs of input and output images, where
the left image in each pair represents the input, and the right image
represents the corresponding output. Each image can be represented as a 2
D matrix: ${matrix}
Please note that each number in the matrix corresponds to a pixel, and
its value represents the color.
[end problem description]

The generated incorrect program fails to solve some example training
input and output pairs in the above problem!

[start incorrect program]
${code}
[end incorrect program]

The incorrect output(s) generated by the incorrect program:
[start incorrect output]
${incorrect_output}
[end incorrect output]

The generated correct output(s):
[start correct output]
${correct_output}
[end correct output]

Please analyze the incorrect reasoning step-by-step, and then generate
the revised program (Python program only), starting with [Start Revised
Program] and ending with [End Revised Program]. Ensure that the revised
program generalizes across different cases and the test input image(s),
while maintaining consistency with the observed input and output image
pairs.

Please include an assert statement with the function signature to verify
that the generated output matches the expected result, starting with [
Assert Statement]. Use placeholders like input_image and output_image for
the variables representing the input and output images.

For example:
[Start Revised Program]
def generate_output_image(input_image):
    rows = len(input_image)
    cols = len(input_image[0])

    def dfs(r, c):
        """Depth-first search to mark all 4-connected '1's to '2's."""
        if r < 0 or r >= rows or c < 0 or c >= cols or input_image[r][c]
        != 1:
            return
        # Change the current component from 1 to 2
        input_image[r][c] = 2
        # Explore neighbors (up, down, left, right)
        dfs(r - 1, c) # Up
        dfs(r + 1, c) # Down
        dfs(r, c - 1) # Left
        dfs(r, c + 1) # Right
```

```

# Traverse the image to find all components with '1'
for r in range(rows):
    for c in range(cols):
        if input_image[r][c] == 1:
            dfs(r, c)
return input_image
[End Revised Program]
[Assert Statement]
assert generate_output_image(input_image) == output_image

Please note, the assert statement should strictly follow the provided
format, and the output image should be represented in list format!
Please note, the script should not include an if __name__ == "__main__":
block.

```

Prompt 7: Refinement with planning-aided code - refinement on both generated plan and code.

===== System =====  
As an expert in analyzing grid-based image processing tasks, your  
objective is to refine your transformation plan and program based on the  
provided feedback.

===== User =====  
The problem description:  
[start problem description]  
The input data consists of a few pairs of input and output images, where  
the left image in each pair represents the input, and the right image  
represents the corresponding output. Each image can be represented as a 2  
D matrix: \${matrix}  
Please note that each number in the matrix corresponds to a pixel, and  
its value represents the color.  
[end problem description]

The generated incorrect transformation plan and program fail to solve  
some example training input and output pairs in the above problem!

[start incorrect transformation plan]  
\${plan}  
[end incorrect transformation plan]  
  
[start incorrect program]  
\${code}  
[end incorrect program]

The incorrect output(s) generated by the incorrect transformation plan  
and program:  
[start incorrect output]  
\${incorrect\_output}  
[end incorrect output]

The generated correct output(s):  
[start correct output]  
\${correct\_output}  
[end correct output]

Please analyze the incorrect reasoning step-by-step, and then generate  
the revised transformation plan (text only) and program (Python program  
only).

For the revised transformation plan, start with [Start Revised  
Transformation Plan] and end with [End Revised Transformation Plan].  
Ensure that the revised transformation plan generalizes across different  
cases and the test input image(s), while maintaining consistency with the  
observed transformations.

For the revised Python program, start with [Start Revised Program] and end with [End Revised Program]. Ensure that the revised program generalizes across different cases and the test input image(s), while maintaining consistency with the observed input and output image pairs.

For the revised Python program, please include an assert statement with the function signature to verify that the generated output matches the expected result, starting with [Assert Statement]. Use placeholders like `input_image` and `output_image` for the variables representing the input and output images.

For example:

[Start Revised Program]

```
def generate_output_image(input_image):
    rows = len(input_image)
    cols = len(input_image[0])

    def dfs(r, c):
        """Depth-first search to mark all 4-connected '1's to '2's."""
        if r < 0 or r >= rows or c < 0 or c >= cols or input_image[r][c] != 1:
            return
        # Change the current component from 1 to 2
        input_image[r][c] = 2
        # Explore neighbors (up, down, left, right)
        dfs(r - 1, c) # Up
        dfs(r + 1, c) # Down
        dfs(r, c - 1) # Left
        dfs(r, c + 1) # Right

    # Traverse the image to find all components with '1'
    for r in range(rows):
        for c in range(cols):
            if input_image[r][c] == 1:
                dfs(r, c)
    return input_image
[End Revised Program]
[Assert Statement]
assert generate_output_image(input_image) == output_image
```

Please note, the assert statement should strictly follow the provided format, and the output image should be represented in list format!

Please note, the script should not include an `if __name__ == "__main__":` block.

#### Prompt 8: Objectness priors augmentation

```
===== System =====
You are an expert in grid-based image analysis.

===== User =====
The training instances consist of several pairs of input and output images, where the left image in each pair represents the input and the right image represents the corresponding output.
Please note that the test instance(s) only contains input image(s).
Each image is represented as a 2D matrix:
${matrix}

Please note that each number in the matrix corresponds to a pixel and its value represents the color.

We treat the color represented by the number {background_color} as the background color.
${abstraction_rule}
```

The components in each input and output image pair are as follows:  
\${component\_description}

Prompt 9: Geometry and topology priors augmentation - component attributes

===== System =====  
You are an expert in geometry and topology analysis. Below is a summary of component attributes, including:  
Size (Width and Height); Color; Shape; Symmetry; Bounding Box; Hole Count; Nearest Boundary.  
===== User =====  
\${geometry\_and\_topology\_priors\_attributes}\$

Prompt 10: Geometry and topology priors augmentation - component relations

===== System =====  
You are an expert in geometry and topology analysis, Below is a summary of component relations, including:  
Different/Identical with other components; Inclusive; Touching or or not touching with other component; Spatial Relations,  
===== User =====  
\${geometry\_and\_topology\_priors\_relations}\$

Prompt 11: Numbers and counting priors augmentation

===== System =====  
You are an expert in numbers and counting analysis. Below is a summary of component statistics, including:  
Symmetry numerical summary; Size numerical summary; Color numerical summary; Shape numerical summary; Hole counting summary.  
===== User =====  
\${numbers\_and\_couting\_priors}\$

Prompt 12: Goal-directedness priors augmentation - action selection

===== System =====  
You are an expert in analyzing and categorizing grid-based image tasks.  
===== User =====  
  
Please determine which category or categories this task belongs to.  
Please select from the following:  
1. color change: color change involves modifying the value of a component, and the component size and position always does not change.  
2. movement: movement involves shifting the position of a component to a new location within the image, and the component size always does not change.  
3. extension: extending involves expanding the boundaries of a component to increase its size or reach within the image, and the component size always changes.  
4. completing: completing an image involves filling in missing or incomplete parts of a component to achieve a coherent and fully formed image.  
5. resizing: resizing involves altering the dimensions of a component by expanding or shrinking its size within the image.  
6. selecting: selecting involves identifying and isolating a specific component within the image as the output component, and the component size and color always does not change.  
7. copying: copying involves duplicating a component and either placing the duplicate in a new location or replacing the existing component within the image.  
8. flipping: flipping involves mirroring a component along a specified axis to reverse its orientation within the image.

9. rotation: rotation involves turning a component around a fixed point or center by a specified angle within the image.  
 10. cropping: cropping involves cutting out a specific portion of a component.

Please select the best suitable one or multiple categories from the provided list that best describe the task.

Format your response by starting with [start category] and ending with [end category], numbering each category selected.

For example, if the task belongs only to "color change", your response should be:

[start category]  
 1. color chang  
 [end category]

If the task belongs to both "selecting" and "extension", your response should be:

[start category]  
 1. selecting  
 2. extension  
 [end category]

Prompt 13: Goal-directedness priors augmentation - target component identification

===== System =====  
 You are an expert in analyzing grid-based image tasks, specifically in \${action} components.  
 ===== User =====  
 If this task involves \${action}:  
 1. Begin by identifying WHICH COMPONENTS are to be \${action} in all input images (training and test pairs).  

- Refer to these components as TARGET components (e.g., component 1 in the first input image, component 2 and component 3 in the second input image, etc.).
- List ALL target components in each training and test input image.
- For EACH target component, provide:
  - Attribute Analysis result
  - Relation analysis result
  - Numerical analysis result

 2. Determine the CONDITIONS used to select these TARGET components for \${action} from each training and test input image.
 

- These conditions must be based on common priorities across all targeted components and must differ from the unselected components.
- For example: the size of all target components might be equal to 3 while the size of the unselected components is not 3.

 2.1. Analyze whether these conditions are EMPTY or not.  
 2.2. Evaluate if these conditions are derived from attribute analysis, including:
 

- 2.2.1. Color
- 2.2.2. Size
- 2.2.3. Shape
- 2.2.4. Width
- 2.2.5. Height
- 2.2.6. The number of holes
- 2.2.7. Bounding box
- 2.2.8. Symmetry
- 2.2.9. Nearest boundary

 2.3. Evaluate if these conditions are derived from relation analysis, including:
 

- 2.3.1. Relative position with other components
- 2.3.2. Touching with other components
- 2.3.3. Whether they differ from or are identical with other components

2.3.4. Enclosure of other components

2.4. Evaluate if these conditions are derived from numerical analysis, including:

- 2.4.1. Symmetry numerical analysis
- 2.4.2. Size numerical analysis
- 2.4.3. Color numerical analysis
- 2.4.4. Shape numerical analysis
- 2.4.5. Hole counting analysis

You must evaluate each condition ONE by ONE and determine the best conditions.

Note:

- The conditions MUST work for ALL training and test input and output image pairs.
- Conditions CANNOT come from the output images!
- A condition can be EMPTY.
- If a condition is based on numerical features (e.g., size (width and height), or the number of holes), you may use the operators =, <, >, >=, or <=.
- For cropping or selecting tasks, consider using a bounding box to extract each component.